2014 년 8 월

박사학위 논문

The study of the microRNA –induced cellular senescence

조선대학교 대학원

의학과

김 옥 현

The study of the microRNA –induced cellular senescence

microRNA에 의한 노인성질환 유발 연구

2014 년 8 월 25 일

조선대학교 대학원

의학과

김 옥 현

The study of the microRNA –induced cellular senescence

지도교수 유 호 진

이 논문을 이학박사학위신청 논문으로 제출함

2014 년 4 월

조선대학교 대학원

의학과

김 옥 현

김옥현의 박사학위논문을 인준함

위원장 조선대학교 교 수 장인엽(인)

위 원 조선대학교 교 수 전제열(인)

위 원 조선대학교 교 수 전영진(인)

위 원 조선대학교 교 수 유호진(인)

위 원 제주대학교 교 수 윤상필(인)

2014년 6월

조선대학교 대학원

CONTENTS

RESULTS

CONTENTS OF FIGURES

국문초록

microRNA에 의한 노인성질환 유발 연구

김 옥 현

지도교수 : 유 호 진

조선대학교 일반대학원

의학과

DNA 손상은 유전자 불안전성을 유발하여 노화를 촉진하고 암을 유발한다. 특히 나이가 들면서 증가하는 암, 관절염, 치매 등은 유전자 손상과 밀접한 연관이 있는데, 아직까지 노화 과정에서 발생하는 유전자 불안전성의 원인에 대해서는 잘 알려져 있지 않다. 본 연구에서는 노화 과정 중에 miR-22 가 증가하고 증가된 miR-22 가 유전자 안정성을 유지하는 MDC1 단백질의 발현을 억제하여 노화된 세포에

서 유전자 불안전성이 증가 사실을 규명하였다. 또한 나이가든 사람과 노화된 쥐의 장에서 miR-22 발현이 증가하고 MDC1 발현이 감소됨을 증명하였으며, 사람 혈액에서 노화가 진행도리 수록 MDC1의 발현이 감소되어 유전자 손상이 증가됨을 규명하였다. 따라서 miR-22는 노인성질환의 예방과 치료에 중요한 타깃으로 향 후 노인성질환 치료제 개발에 기여 할 수 있을 것으로 판단된다.

INTRODUCTION

Repeated exposure to both exogenous and endogenous insults challenges the integrity of cellular genomic material. Eukaryotes have evolved a system called the DNA damage response (DDR), which allows cells to sense DNA damage and orchestrate the appropriate cell-cycle checkpoints and DNA repair mechanisms (1). The failure to respond to DNA damage is a characteristic associated with genomic instability and with the onset of diseases, including neurodegenerative diseases, immune deficiency, cancer, and premature aging (2).

DNA double-strand breaks (DSBs) activate the DDR by triggering the kinase activity of ataxia telangiectasia mutated (ATM), thereby initiating a signaling cascade in which the histone variant H2AX (γ-H2AX), located at DSB sites, becomes phosphorylated, and other DDR factors, including the adaptor protein Mediator of DNA Damage Checkpoint 1 (MDC1), are recruited. MDC1 amplifies the ATM signaling activity, leading to a higher percentage of phos-

phorylated H2AX proteins and contributing to the recruitment and retention of additional DDR factors at the sites of DNA damage (3). Thus, MDC1 has been termed a master regulator, modulating the specific chromatin microenvironment required to maintain genomic stability. MDC1 knockout mice show chromosomal instability, defective DNA repair, and radiation sensitivity (4). Furthermore, loss of MDC1 is associated with an increased occurrence of tumors in mice (5), and reduction or lack of MDC1 has been observed in breast and lung carcinoma cells in humans (6). Therefore, cellular levels of MDC1 appear to impact genomic instability and tumorigenicity directly. Although post-translational modification via small ubiquitin-like modifiers affects the stability of MDC1 and its function in DDR (7-9), little is known about how the expression of MDC1 is regulated and which pathophysiological conditions are associated with this regulation.

MicroRNAs (miRNAs) are small noncoding RNAs, consisting of ~22 nucleotides, that suppress protein synthesis, usually by interacting with the 3-untranslated region (3′-UTR) of target mRNAs (10). Several lines of evidence suggest that miRNAs negatively regulate the expression of DDR proteins, decreasing the capacity for DSB repair and increasing radiosensitivity (11-14). In addition, impairment of miRNA processing through the inactivation of DICER or DROSHA results in a lack of DDR factor recruitment to DSB sites (15). Therefore, miRNAs may play an important role in the regulation of DDR, and may contribute to the maintenance of genomic integrity.

In this study, we explored the regulation of MDC1 expression and the subsequent effects on DDR and genomic integrity. We found that miRNA-22 (miR-22) down-regulated MDC1 expression, leading to impaired response to DNA damage, decreased DSB repair, and increased genomic instability. Up-regulation of endogenous miR-22 expression under several pathophysiological

conditions led to the accumulation of DNA damage through down-regulation of MDC1. Thus, miR-22 plays a crucial role in the regulation of MDC1 expression and presents a new mechanism by which cancer can occur.

MATERIALS AND METHODS

1. Cell cultures and treatment.

Human cervical carcinoma HeLa and Si-Ha cells, human osteosarcoma U2OS cells and human embryonic kidney HEK293T cells were cultured in Dulbecco's modified Eagle's medium (DMEM) supplemented with 10% heat-inactivated fetal bovine serum (FBS, Lonza), 100 units/ml penicillin and 100 g/mL streptomycin (Invitrogen). HCT116 colorectal carcinoma cells were grown in Iscove's modified Dulbecco's medium (IMDM) containing 10% FBS, penicillin and streptomycin. The human breast adenocarcinoma MCF7 and MDA-MB-231 cells were cultured in RPMI-1640 medium containing 10% FBS, penicillin and streptomycin. The human embryonic lung fibroblasts MRC-5 and IMR-90 cells were maintained in Earle's MEM containing 10% FBS, penicillin and streptomycin. MRC-5 and IMR-90 cells at early passages (10-20 passages) were used in all experiments because two human primary fibroblasts cells have a mean lifespan of ap-

proximately 50-60 population doublings. All cell lines were from the American Type Culture Collection (ATCC). To induce DNA double strand breaks, expo-nentially growing cells were irradiated at 10 Gy from 137Cs source (Grammacell 3000 Elan irradiator, Best Theratronics) and were allowed to recover at 37 C for the indicated times. For terminal differentiation, MCF7 cells were treated with 12-O-tetradecanoylphorbol-13-acetate (TPA, Sigma) at 100 nM for 3 days. For induction of senescence, cells at approximately 70-80% confluence were treated with 150 M H2O2 (Sigma) or 120 M Busulfan (Sigma) for 2 hr or 24 hr, respectively. The cells were washed with PBS to remove reagents and placed in fresh media for 6-7 days.

2. miRNA and plasmid transfection.

Has-miR-22 duplex and negative control miRNA were purchased from Bioneer. Cells were transfected with 50 nM miRNA using lipofectamine RNAiMax (Invitrogen) according to the manufacturer's instructions. For rescue experi-

ments, the pcDNA-HA-MDC1 construct (a gift from Zhenkun Lou, Mayo Clinic, Rochester, MN), CA-Akt1 (Millipore, Billerica, MA), and miR-22 inhibitor (anti-miR-22, miR-22 antisense-oligonucleotide (ASO), Panagene) were used. pcDNA-HA empty vector and scrambled oligonucleotide were used as a negative control. To analyze Akt1-mediated miR-22 regulation, a CA-Akt1 expression plasmid was used. Cells were first transfected with 50 nM miR-22 for 4-6 hr using lipofectamine RNAiMax, and sequentially transfected with 1 g of pcDNA-HA-MDC1, CA-Akt1 vector or 50 nM miR-22 inhibitor using lipofectamine 2000 reagent (Invitrogen) according to the manufacture's instructions. The cells were harvested 48 hr later.

3. Antibodies.

Polyclonal MDC1 antibody (R2) was raised in rabbit against a GST fusion protein containing the BRCT domain of MDC1 (residues 1882-2089). The MDC1 protein was detected using western blot analysis with rabbit polyclonal MDC1

antibody (R2) or anti-MDC1 polyclonal antibody (Ab11170, Abcam) at a 1:2000 or 1:1000 dilution, respectively. and DNA damage foci of MDC1 were also detected by immunofluorescence staining using the anti-MDC1 rabbit polyclonal antibody (R2) at a 1:200 dilution. The following antibodies were used for western blot analysis: anti-53BP1 mouse monoclonal antibody (1:1000, BD), anti-Akt1 rabbit polyclonal antibody (1:1000, Cell Signaling Technology), anti-phospho Akt1 (Ser473) rabbit polyclonal antibody (1:1000, Cell Signaling Technology), anti-ATM mouse monoclonal antibody (1:2000, AbFrontier), and anti- -Tubulin mouse monoclonal antibody (1:5000, Santa Cruz). The following antibodies were used for immunofluorescence staining: anti- -H2AX mouse monoclonal antibody (1:200, JBW301, Upstate). For immunohistochemistry, anti-MDC1 polyclonal antibody (Ab11170, Abcam) and anti-phospho Akt1 (Ser473) rabbit polyclonal antibody (Cell Signaling Technology) were used.

4. Western blot analysis.

Cells or mouse tissues were lysed in ice-cold RIPA buffer [50mM Tris-HCl (pH 7.5), 150mM NaCl, 1% Nonidet P-40, 0.5% sodium deoxycholate, 0.1% sodium dodecyl sulfate, 1mM dithiothreitol, 1mM phenylmethanesulfonyl fluoride, 10 g/ml leupeptin and 10 g/ml aprotinin]. Equal amounts of cell or tissue extracts were separated by 6-12% SDS-PAGE followed by electrotransfer onto a polyvinylidene difluoride membrane (Pall Life Sciences). The membranes were blocked for 1 hr with TBS-t [10mM Tris-HCl (pH 7.4), 150mM NaCl and 0.1% Tween-20] containing 5% nonfat milk and then incubated with indicated primary antibodies overnight at 4 C. The blots were washed four times for 15 min with TBS-t and then incubated for 1 hr with peroxidase-conjugated secondary antibodies (1:5000, Jackson ImmunoResearch Inc). The blots were washed four more times with TBS-t and developed using an enhanced chemiluminescence detection system (ECL, Intron). The amount of MDC1 protein was quantified using Scion Image software (Scion Corp.)

5. Immunofluorescence microscopy.

To visualize DNA damage foci, cells cultured on cover slips coated with poly-L-lysine (Sigma) were irradiated at 10 Gy and allowed to recover at 37 C for adequate times. Cells were washed twice with PBS and fixed with 4% paraform-aldehyde for 10min and ice-cold 98% methanol for 5 min, followed by permeabilization with 0.3% Triton X-100 for 10 min at room temperature. After permeabilization, coverslips were washed three times with PBS and then were blocked with 5% BSA in PBS for 1 hr. Cells were single or double immunostained with primary antibodies against the indicated proteins overnight at 4 C. Cells were washed with PBS and then stained with appropriate Alexa Fluor 488- (green, Molecular Probe), Alexa Fluor 594- (red, Molecular Probe) conjugated secondary antibodies. After washing, the coverslips were mounted onto slides using Vectashield mounting medium with 4,6 diamidino-2-phenylindole (Vector Laboratories, Burlingame, CA). Fluorescence images were taken using a confocal

microscope (Zeiss LSM 510 Meta; Carl Zeiss) and analyzed with Zeiss micro-scope image software ZEN (Carl Zeiss). For foci quantification experiments, cells with > 5 foci were counted as MDC1 or -H2AX foci-positive cells by randomly selecting at least 100 cells and the percentage was calculated by di-viding the number of foci positive cells with the number of DAPI-stained cells. The error bars represent the standard error from three independent experiments.

6. RNA extraction and Quantitative real-time PCR (qRT-PCR).

Total RNA was isolated from cultured cells and mouse tissues using TRIzol (Invitrogen) according to the manufacturer's protocol. For quantitation of mdc1 mRNA and pre-miR-22, cDNA was synthesized using 1 μg of total RNAs, ran-dom hexamer (Promega) and M-MLV reverse transcriptase (Invitrogen). Real-time PCR analysis was performed using the SYBR green-based fluorescent method (SYBR premix Ex Taq kit, TaKaRa Bio) and the MX3000P® qRT-PCR system (Stratagene) with specific primers. Primers used for real-time PCR are

as follows: mdc1 forward, 5 -tgctcttcacaggagtggtg-3 and mdc1 reverse, 5 -gggcacacaggaacttgact-3 ; pre-miR-22 forward, 5 -ctgagccgcactagttcttc-3 and pre-miR-22 reverse, 5 -ggcagagggcaacagttctt-3 ; gapdh forward, 5 -ttcaccaccatggagaaggc-3 and gapdh reverse, 5 -ggcatggactgtggtcatga-3 . To quantify miRNAs, cDNA was synthesized using Mir-XTM miRNA first-strand synthesis and SYBR qRT-PCR kit (Clontech) according to the manufacturer's instructions. Briefly, in a single-tube reaction, RNA molecules are polyadenylated and reverse transcribed using poly(A) polymerase and SMART™ MMLV Reverse Transcriptase. The SYBR Advantage® qPCR Premix and mRQ 3′ Primer are then used in real-time qPCR, along with miRNA-specific 5′ primers. hsa-miR-22- MIMAT0000077, hsa-miR-98-MIMAT0000096, miR-124-MIMAT0000422, miR-125a- MIMAT00004223 and mmu-miR-22-MIMAT0000531 were used as primers for real-time qPCR. The quantity of transcripts was calculated based on the threshold cycle (Ct) using the delta-

delta Ct method that measures the relative of a target RNA between two samples by comparing them to a normalization control RNA (gapdh or U6).

7. Luciferase assay.

A segment of the 3′-UTR of MDC1 (a 658 bp fragment starting after the TGA stop codon) containing the putative miR-22 binding site was cloned into pMIR-REPORT luciferase vector (Applied Biosystems). A deletion mutant of the miR-22 binding site was made using the GENEART Site-Directed Mutagenesis kit (Invitrogen). Primers used for mutagenesis were as follows: forward primer 5′-tgctcagatgtcataagtgatctttagccagactgttg-3′ and reverse primer 5′-caacagtctggctaaagatcacttatgacatctgagca-3′. For the luciferase activity assay, the pMIR-REPORT firefly luciferase vector containing 3′-UTR of MDC1 WT (wild type) or MT (mutant) and pRL-TK vector containing Renilla luciferase as a control were co-transfected into cells using Lipofectamine 2000 (Invitrogen), and sequentially transfected with miR-22, anti-miR-22 or CA-Akt1 vector.

After 24 hr of transfection, the luciferase assay was performed using the dual luciferase reporter assay system (Promega) according to the manufacturer's instructions. Luciferase activity was quantified using a luminometer (Glomax, Promega). The luciferase activity data were normalized to the Renilla value, and the results were represented as the average and standard deviation (sd) from triplicate of experiments.

8. Extraction of RNA and protein from mouse tissues.

The mouse lung (n=5) and colon tissues (n=5) were obtained from the Aging Tissue Bank (ATB), a member of the National Biobank of Korea. Tissues were homogenized in TRIzol (Invitrogen) and RIPA buffer according to the manufacturer's protocol for extraction of RNA and protein, respectively.

9. Immunohistochemistry.

The tissue microarray slides include human prostate cancer tissues taken form Super Bio-Chips (SuperBioChips Laboratories, Seoul, Republic of Korea). The

young and senescent colon tissues were obtained from the Chosun University Department of Pathology tissue bank. The endogenous peroxidase activity was blocked with 0.03% H2O2 and the non-specific binding was suppressed by incubation with 10% normal horse serum (Vector Laboratories). The specimens were incubated with rabbit anti-pAkt1 or anti-MDC1 polyclonal antibodies, diluted at 1:1000, for 24 hr at 4 C. The primary antibody binding was visualized using an avidin-biotin-peroxidase kit (Vectastain ABC kit) according to the manufacturer's instructions. The sections were incubated with biotinylated goat anti-rabbit IgG at 1:200 dilution and then the ABC complex, for 1 hr each. Labeling was visualized by incubating 0.05% 3',3-diaminobenzidine (DAB; Sigma-Aldrich) and 0.01% H2O2 for 5-15 min. The sections were dehydrated through a graded ethanol series, cleared with xylene and mounted under Polymount (Shandon). Omission of incubation with the primary antibody served as a control for the false positive immunoreaction. Immuno-labeled images were directly

captured using an Olympus C-4040Z digital camera and an Olympus BX-50 microscope (Olympus Corp.). The captured images were saved and subsequently processed using Adobe Photoshop (Adobe System). The brightness and contrast of images were adjusted only for the purpose of background consistency.

10. Chromosomal aberration analysis.

For chromosomal analysis, indicated transfected-U2OS cells were treated with 1 Gy of -ray for 24 hr. To arrest cells in metaphase, 300 ng/ml colcemid (Sigma) was added 4 hr before cell harvest. Colcemid depolymerizes microtubules and inhibits the formation of the mitotic spindle. Cell were harvested in 15 mL tubes, gently resuspended in 40% of culture media for 10 min at 37℃, and then fixed in equivalent volume of a freshly prepared fixative solution (3:1 mixture of methanol/acetic acids, Carnoy's solution). After removal of supernatant, pellets were resuspended in fixative solution, dropped onto a cleaned glass slide and air-dried overnight. The slide was mounted in Vectashield with DAPI (Vec-

tor Laboratories). Metaphase images were captured using a confocal microscope (Zeiss LSM 510 Meta; Carl Zeiss) and analyzed with the Zeiss microscope image software ZEN (Carl Zeiss).

11. DR-GFP assay (HR assay).

U2OS-DR-GFP cells were transfected with control or CA-Akt1 vector using lipofectamine 2000, and sequentially transfected with miR-22 inhibitor, and then infected with I-SceI-carrying adenovirus at an estimated MOI of 10. After 72 hr, GFP-positive cells were measured by fluorescence-activated cell sorting (FACSCalibur, BD Biosciences). The acquired data was analyzed using CellQuest Pro software (BD Biosciences). The data are presented as the mean s.d. value for three independent experiments.

12. SA-β-gal (Senescence Associated-galactosidase) assay.

SA-β-gal activity was determined using the Senescence Cells Histochemical Staining Kit (Sigma) according to the manufacturer's protocols. Briefly, cells

were washed with 1X PBS, fixed with 1X fixation buffer and incubated in staining solution containing X-gal at 37℃ without CO2 until the cells stained blue (2 hr to overnight). Senescent cells were defined as those that appeared blue when viewed under a light microscope. A minimum of 1000 cells in randomly chosen fields were used to calculate the percentage of SA-β-gal positive cells.

13. Single cell gel electrophoresis (Comet) assay.

Comet assay was done by alkaline single-cell agarose gel electrophoresis as described previously (60). Briefly, cells were treated with 10 Gy of -ray, fol- lowed by incubation in culture medium at 37 C. Cells were then harvested (20 l, 1 105 cells per pellet), mixed with 200 l low-melting agarose and lay- ered onto agarose-coated glass slides. The slides were maintained in the dark at 4 C for all subsequent steps. The slides were immersed in lysis solution [2.5 mol/L NaCl, 100 mmol/L Na2EDTA, 10 mmol/L Tris-HCl (pH 10), containing freshly added 1% Triton X-100 and 10% DMSO] for 1 hr at 4 C and then

placed into a horizontal electrophoresis apparatus filled with fresh alkaline elec-trophoresis buffer [1 mmol/L Na2EDTA, 300 mmol/L NaOH (pH >13)]. After electrophoresis (30 min at 1V/cm tank length), air-dried and neutralized slides were stained with ethidium bromide (20 g/ml) overnight, and kept in a moist chamber in the dark at 4 C until needed. The slides were analyzed at 400X magnification using a fluorescence microscope (Nikon). The microscope images revealed circular shapes, indicating undamaged DNA, or comet-like shapes, in-dicating the DNA had migrated out from the head to form a tail (damaged DNA). Average comet tail moment was scored for 40-50 cells/slide using a computer-ized image analysis system (Komet5.5, Andor Technology).

14. Clonogenic survival assay.

After treatment with irradiation (IR), 5 102 cells were immediately seeded on 60mm dish in triplicate and grown for 2-3 weeks at 37 C to allow colonies to form. Colonies were stained with 2% methylene blue/50% ethanol and were

counted. The fraction of surviving cells was calculated as the ratio for the plating efficiency of treated cells over untreated cells. Cell survival results are reported as the mean value ± s.d. for 3 independent experiments.

15. BrdU incorporation assay.

For the analysis of irradiation-induced S-phase cell cycle checkpoint, the incorporation of bromodeoxyuridine (BrdU) was monitored as a parameter for DNA synthesis, according to the manufacturer's instructions (Roche Diagnostic Corp.). Briefly, cells were treated with the indicated gray of -ray. After 2 hr, 10 μM BrdU was added to the culture medium for 2 hr at 37℃ for incorporation into freshly synthesized DNA. After fixation of the cells, cellular DNA was partially digested by nuclease treatment. A peroxidase-labeled antibody against BrdU and a peroxidase substrate were added sequentially to yield colored reaction products, which are proportional to the level of BrdU incorporation into the cellular DNA. Colored products were measured using a microplate reader at 405

nm with a reference wavelength at approximately 490 nm. The relative DNA synthesis was calculated as the percentage of absorbance of cells treated with irradiation from the absorbance of untreated cells. The data are represented as the average ± s.d. value from experiments performed in triplicate.

16. Isolation of mononuclear cells from human blood.

Blood samples were provided by the Kwang-San Health Center (Gwangju, Republic of Korea). Blood donors were healthy men or women in their twenties (n=7) or sixties (n=11). The protocol for human studies was approved by the Institutional Review Board of Chosun University School of Medicine. Human blood samples were collected in a tube containing heparin as an anticoagulant. The peripheral blood mononuclear cells (PBMCs) were extracted from the blood using LymphoprepTM (Axis-Shield), and total RNA was purified using TRIzol (Life Technologies). Briefly, in the Lymphoprep protocol, blood was diluted with 0.9% NaCl (1:1), and isolated by density gradient centrifugation at 800g for 20

min using Lymphoprep. The collected mononuclear cells were washed twice with PBS and then used for experiments.

17. CGH array and data analysis.

Human fibroblast GM00637 cells were stably transfected with control miRNA or miR-22, and genomic DNA was isolated using AccuPrep Genomic DNA Extraction kit (Bioneer) according to the manufacturer's instructions. Array CGH analysis was performed using the Nimblegen Human CGH 12 135K whole-genome tiling v3.1 Array (Agilent Technologies). Human genomic DNA (1 g) from miR-22-tranfected cells and reference DNA samples from control cells were independently labeled with fluorescent dyes (Cy3/Cy5), co-hybridized at 65 C for 24 hr, and then subjected to the array. The hybridized array was scanned using NimbleGen MS200 scanner (NimbleGen Systems Inc.) with 2 m resolution. Log2-ratio values of the probe signal intensities were calculated and plotted versus genomic position using Roche NimbleGen NimbleScan v2.5 soft-

ware. Data are displayed and analyzed in Roche NimbleGen SignalMap software and CGH-explorer v2.55.

18. Statistical analysis.

Data in all experiments are represented as mean s.d. Statistical comparisons were carried out using two-tailed paired t-test. We considered p 0.01(**) as significant. Analyses were carried out with Prism software (GraphPad) and Excel (Microsoft). Negative correlation of MDC1 expression with pAkt1 levels was assessed using the Pearson correlation test with p value. p values less than or equal to 0.01 were considered statistically significant.

RESULT

1. MDC1 expression is post-transcriptionally regulated by miR-22.

To explore the possibility that MDC1 expression could be regulated at the post-transcriptional level, we carried out a comprehensive bioinformatics analysis to generate a selective miRNA library that could then be used for screening. From this analysis, a total of 8 miRNAs were identified as candidates (Supplemental Table 1) and each was reversely screened for the effect on MDC1 expression by using a luciferase assay. Specifically, the 3 -UTR of MDC1, the region with the highest potential to contain miRNA binding sites, was cloned into the luciferase vector pMIR-REPORT. This construct (MDC1 3 -UTR-wt) was cotransfected into HEK293T cells along with either a control miRNA (miR-Ctrl) or with one of the candidate miRNAs. The results of the luciferase assays revealed that overexpression of miR-22 led to remarkably lower luciferase activity compared with control miRNA (Figure 1A). On the

other hand, other miRNAs could not be strong enough to repress luciferase activity. Western blotting analysis also revealed that the MDC1 protein level was significantly decreased in cells transfected with miR-22, whereas others had no effect (Figure 1B). The TargetScan algorithm (MIT, release 6.2) showed that bases 317-339 in the MDC1 3 -UTR are complementary to the target sites of miR-22 (Figure 1C). To investigate this further, we constructed a mutated MDC1 3 -UTR luciferase reporter (MDC1 3 -UTR-mt) that was lacking predicted seed region for the miR-22. We found that co-transfection of the wild-type reporter construct, but not mutant, with miR-22 or its premature hairpin (pre-miR-22) led to suppression of luciferase activity (Figure 1D). Furthermore, when a miR-22 antisense oligonucleotide (anti-miR-22) was added in addition to miR-22 or pre-miR-22, luciferase activity was restored to control levels (Supplemental Figure 1A), indicating that miR-22 targets the 3 -UTR of MDC1 mRNA. Consistent with these results, the

MDC1 expression level decreased as the concentrate of transfected miR-22 or pre-miR-22 was increased (Supplemental Figure 1B). Moreover, when miR-22 was transfected into HeLa or U2OS cells, there was a significant decrease in MDC1 protein levels specifically (Supplemental Figure 1C). Using real-time quantitative PCR (qPCR), we observed that MDC1 mRNA was reduced more than 50% when miR-22 was overexpressed (Supplemental Figure 1D).

We then exposed cells to ionizing radiation (IR) to induce DNA damage, and performed immunofluorescence to look for the formation of MDC1 foci. When miR-22 was transfected into either U2OS or HeLa cells, there were significantly fewer visible foci than in the control cells (Supplemental Figure 2A). In the control, the percentage of cells with 5 MDC1 foci continued to increase over time, whereas in the miR-22-transfected cells, the percentage containing 5 MDC1 foci remained low. Importantly, MDC1 foci formation in cells transfected with miR-22 was fully restored when either anti-miR-22 (Figure 1E

and Supplemental Figure 2B) or a miR-22-insensitive MDC1 was introduced (Figure 1F and Supplemental Figure 2C). Taken together, these results suggest that MDC1 expression is post-transcriptionally regulated by miR-22.

2. miR-22 affects DDR function of MDC1 and induces genomic instability.

Next, we asked whether the miR-22 regulation of MDC1 was physiologically relevant to DDR. Because MDC1 directly regulates DSB repair through homologous recombination (HR) (16) and non-homologous end joining (NHEJ) (17), we asked whether the regulatory effects of miR-22 would lead to DSB repair phenotypes as well. To test this hypothesis, we exposed miR-22-transfected U2OS and HeLa cells to IR and then measured DSB repair using either -H2AX immunofluorescence staining or single-cell electrophoresis (comet assay). Cells transfected with miR-22 had significantly more residual DSBs than control cells, as evidenced by the increase in signal intensity of -

H2AX staining and by the increase in comet tail moments (Figure 2, A and B). Co-transfection with anti-miR-22 (Figure 2A and Supplemental Figure 2B) or with miR-22-insensitive MDC1 (Figure 2B and Supplemental Figure 2C) reversed this effect, suggesting that this defect in DSB repair can be rescued by interrupting the interaction between miR-22 and the MDC1 3 -UTR.

MDC1 also plays a role in the regulation of an intra-S-phase cell cycle checkpoint in response to DNA damage and contributes to the sensitivity of cells to DNA-damaging agents (18-20). Thus, we asked whether the presence of miR-22 would also affect this particular role of MDC1. As shown in Figure 2C, miR-22 abrogated IR-induced S-phase checkpoint, as cells transfected with miR-22 has a higher percentage of BrdU incorporation than cells transfected with miR-Ctrl. Furthermore, up-regulation of miR-22 made cells hypersensitive to IR treatment and decreased the cell survival rate (Figure 2D). These detrimental effects were fully rescued by overexpressing miR-22-

insensitive MDC1, emphasizing the importance of MDC1 in this process.

Frequent DSBs and continued DNA synthesis in the presence of DNA damage increase the risk of genomic instability. Thus, we predicted that miR-22 would have an effect on genomic instability. Indeed, overexpression of miR-22 in U2OS cells significantly increased the number of chromosome breaks after IR exposure as compared to control cells (Figure 2E). In contrast, anti-miR-22 or miR-22-insensitive MDC1 transfection into miR-22-expressing cells completely restored chromosome breaks. To assess the subsequent genomic effects resulting from the numerous chromosomal breaks in miR-22-expressing cells, we performed array comparative genomic hybridization (ar-ray CGH) using human fibroblast GM00637 cells. From this analysis, we con-clude that there was a high frequency of chromosomal abnormalities, including clonal amplifications and deletions in discrete regions (Figures 2F and Supple-mental Figure 3). Taken together, these results provide evidence that miR-

22-mediated down-regulation of MDC1 results in defects in DSB repair, and allows cells to bypass an intra-S-phase checkpoint causing a decrease in chromosome integrity.

3. Akt1 up-regulates endogenous miR-22 and inhibits homologous recombination.

The oncogenic potential of Akt1 lies in its ability to repress homologous recombination (HR) and thereby cause genomic instability (21). Because it has been shown that Akt1 activates miR-22 expression in human cancer cells (22, 23), we hypothesized that the subsequent down-regulation of MDC1 that results from a stimulation of miR-22 expression is the underlying reason for the repression of HR. Overexpression of constitutively active Akt1 (CA-Akt1) in either U2OS or HCT116 cells led to increased miR-22 expression and decreased MDC1 protein and mRNA levels (Figure 3A and Supplemental Figure

4A). Under these same conditions, IR-induced formation of MDC1 foci decreased significantly (Supplemental Figure 4B). To confirm the role of miR-22 in this process, we showed that co-transfection with anti-miR-22 rescued MDC1 expression (Figure 3B) and restored MDC1 foci formation (Figure 3C). Moreover, the luciferase activity of the MDC1 3 -UTR was decreased in the CA-Akt1-overexpressing cells. However, overexpression of CA-Akt1 had no effect on the luciferase activity of the mutated MDC1 3 -UTR (Supplemental Figure 4C). Together, these results suggest that increased levels of miR-22, either through transfection or endogenously in response to Akt1, targets the same regulatory network and leads to the same DDR phenotype.

To test the hypothesis that MDC1 levels are central to the observed effects of Akt1 on HR, we examined HR efficiency using a green fluorescent protein (GFP)-based chromosomal assay. This assay monitors HR-mediated repair of DSB generated by ectopically expressed I-Sec I endonuclease in GFP con-

struct (24). When DSBs are repaired by HR, GFP is expressed and levels can be quantitated using flow cytometry (Figure 3D). We established a stable cell line using U2OS cells (U2OS DR-GFP) and monitored HR-mediated DSB repair by measuring GFP levels. We found that the GFP signal decreased drastically in cells expressing CA-Akt1 and were restored to normal levels in cells co-transfected with either anti-miR-22 (Figure 3E) or miR-22-insensitive MDC1 (Figure 3F and Supplemental Figure 4D), implying that MDC1 expression levels, signaled by Akt1 and mediated through miR-22, are important in HR-mediated DSB repair.

Because pAkt1 levels correlate with miR-22 expression in prostate tumor tissues (23), we used this system to ask whether Akt1 activity directly affects MDC1 levels in vivo. A prostate tumor tissue array was used to examine the correlation between MDC1 and pAkt1 level by immunohistochemistry. We found that specimens with strong MDC1 staining had weak pAkt1 signals and

vice versa (Figure 3, G and H), confirming a statistically significant inverse correlation between MDC1 and pAkt1 levels (Figure 3I).

4. Cellular differentiation up-regulates endogenous miR-22 and suppresses DSB repair.

It is known that miR-22 levels increase in terminally differentiated cells (14, 25, 26). Therefore, we predicted that miR-22 expression in differentiated cells directly affects DSB repair. Because 12-O-tetradecanoylphorbol-13-acetate (TPA) causes breast cancer MCF-7 cells to become post-mitotic (27), we used this system to enrich for terminally differentiated cells and monitored endogenous miR-22 and MDC1 levels. After 3 days of differentiation in response to TPA, miR-22 levels increased more than 2-fold and MDC1 levels decreased accordingly (Figure 4A and Supplemental Figure 5A), confirming an inverse correlation between the two during cellular differentiation. We then

used this same system to assess effects on IR-induced MDC foci and DSB repair. When untreated MCF-7 cells were exposed to IR, clearly visible MDC1 foci formed, and the number of cells with foci continued to increase for three hr after exposure (Supplemental Figure 5B). In contrast, cells that were stimulated to differentiate through TPA treatment had little or no MDC1 foci formation after exposure to IR. However, when TPA-differentiated MCF-7 cells were transfected with anti-miR-22, MDC1 expression (Figure 4B) and IR-induced MDC1 foci formation (Figure 4C) were recovered. Moreover, using comet assays and -H2AX staining, we observed that an impaired DSB repair capacity in differentiated cells was also improved significantly by anit-miR-22 (Figure 4D) or miR-22-insensitive MDC1 (Figure 4E and Supplemental Figure 5C). Together, these results provide evidence that endogenous miR-22 induced in response to cellular differentiation affects DSB repair, and suggest that miR-22-mediated down-regulation of MDC1 is an important pathway af-

fecting genomic instability in terminally differentiated cells.

5. Senescence-induced up-regulation of endogenous miR-22 affects DSB repair.

Recently, miR-22 expression was shown to increase during replicative senescence of human fibroblasts (28). Because DNA damage and mutations accumulate during aging in mammals (29), we hypothesized that down-regulation of MDC1 is relevant in this process also, and we examined the levels of miR-22 and MDC1 during both replicative senescence and premature stress-induced senescence. Senescence was induced in both human embryonic lung fibroblasts MRC-5 and IMR-90 cells by either serial passaging or by treatment with either hydrogen peroxide (H2O2) or busulfan (BU). We defined senescent cells as late-passage, non-proliferating cells at a population doubling level (PDL) of ~55 and young cells as early-passage, proliferating cells (~20

PDL). Senescent MRC-5 and IMR-90 cells adopted the predicted morphology, flat and enlarged, and they stained positively for -galactosidase, an enzyme that is specifically induced in senescent cells (SA- -gal) (Figure 5A, upper panel). Levels of miR-22 were markedly higher in senescent cells than in young cells for all three cell populations: replicatively senescent and H2O2-induced prematurely senescent cells (Figure 5A, lower panel), as well as BU-induced prematurely senescent cells (Supplemental Figure 6A). Consistent with our previous results, high levels of miR-22 in senescent cells were accompanied by significantly lower levels of MDC1 (Figures 5B and Supplemental Figure 6B) and fewer IR-induced MDC1 foci than in young cells (Supplemental Figure 6, C and D). When senescent cells were transfected with anti-miR-22, the level of MDC1 (Figure 5C) and the number of IR-induced MDC1 foci (Figure 5D) were equivalent to those of young cells.

The levels of several components of the HR complex, including Rad51,

Rad51C, and NBS1, decrease as cells age (30). Supplementing pre-senescent cells with these proteins, either individually or in combination, does not rescue a defect in DSB repair (30), suggesting that other factors in this regulatory pathway account for the impaired DSB repair activity in senescent cells. Based on our results thus far, we reasoned that the regulation of MDC1 expression determines the amount of DSB repair in senescent cells. To test this, we introduced either anti-miR-22 or miR-22-insensitive MDC1 into senescent cells and examined the effect on DSB repair. Young cells that were exposed to IR repaired the majority of DSBs within 6 hr, as measured by the percentage of comet tail moments (Supplemental Figure 7A). In contrast, senescent cells still had numerous unrepaired DSBs 6 hr after IR exposure, but this effect was reversed if anti-miR-22 was present (Figure 5E). The DSB repair defect in senescent cells was also fully rescued by overexpressing miR-22-insensitive MDC1 (Figure 5F and Supplemental Figure 7B). These results suggest that

miR-22 acts to regulate DSB repair in senescent cells by modulation expression of MDC1.

Because there was an inverse relationship between miR-22 and MDC1 levels in senescent cells, we predicted that the same effect would be true of the aging process in human and mouse tissues. To test this prediction, we measured miR-22 and MDC1 expression levels in lung and colon tissues from young and old mice using real-time qPCR and western blotting. For both lung and colon tissues, the older mice had higher levels of miR-22 (Figure 6A) and lower levels of MDC1 (Figure 6B) than younger mice. Based on our previous observations, it is very likely that the decreased MDC1 levels in lung and colon tissues in older mice were a direct result of the high levels of miR-22. We were able to show the same effect in human cells using peripheral blood mononuclear cells (PBMCs) from young (n = 7) and old (n = 11) human donors (Figure 6C). Furthermore, the same was true for human tissue samples. When colon

biopsies from young (17 and 24 years old) and old (64 and 68 years old) donors were subjected to immunohistochemical analysis, staining for MDC1 was much darker in younger colon tissue than the older tissue, again showing that MDC1 abundance decreases with aging (Figure 6D). Thus, miR-22 mediated down-regulation of MDC1 expression is a common mechanism in aging cells and is utilized in diverse and widespread tissue types in mammals.

6. miR-22 expression induces a senescence-like phenotype in human cancer cells and leads to the accumulation of DNA damage.

Senescence includes an irreversible cell-cycle arrest that has therefore been proposed to inhibit tumorigenesis (31). Several studies have proposed that miR-22 is a tumor suppressor because it induces senescence-like phenotypes in cancer cells and it triggers both growth suppression and apoptosis (28, 32-35). However, our data highlight a previously unknown oncogenic

function of miR-22, in that it inhibits DSB repair and consequently increases the risk of genomic instability, a hallmark of cancer cells. Thus, we examined whether DNA damage accumulation accompanied miR-22-induced cellular senescence in cancer cells. To this end, we introduced miR-22 into human breast cancer cells (MCF7 and MDA-MB-231) and human cervical cancer cells (si-Ha) and measured the accumulation of unrepaired DSBs after IR exposure. Consistent with a previous report (28), introduction of miR-22 into cancer cells caused a senescence-like phenotype, as observed by the increased SA--gal activity (Supplemental Figure 8). Intriguingly, miR-22-induced senescent cells showed a dramatic reduction in MDC1 expression (Figure 6E) and a significant increase in the number of unrepaired DSBs as compared to control cells (Figure 6F). Moreover, when miR-22-induced senescent cells were transfected with miR-22-insensitive MDC1, there were significantly fewer DSBs (Figure 6F). These results are consistent with our working model, in

which the miR-22-mediated decrease in MDC1 plays a central role in the ac-

cumulation of DSBs in senescent cells.

Figure 1

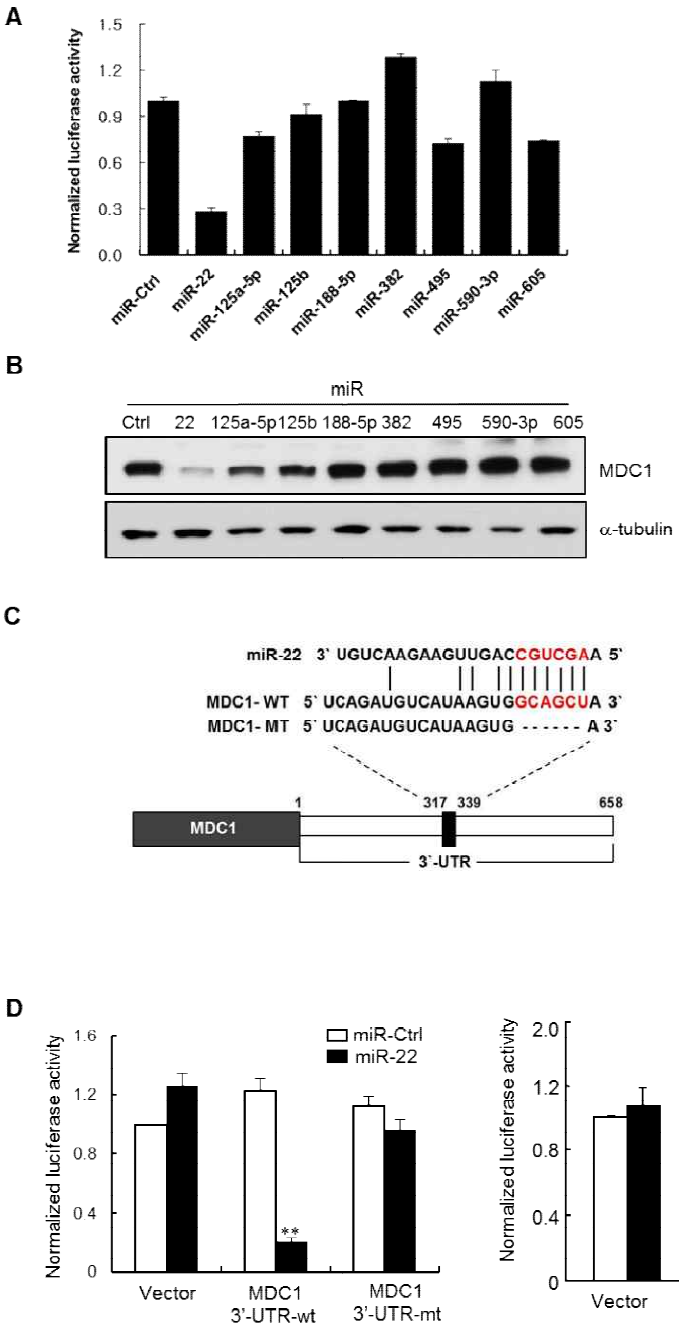

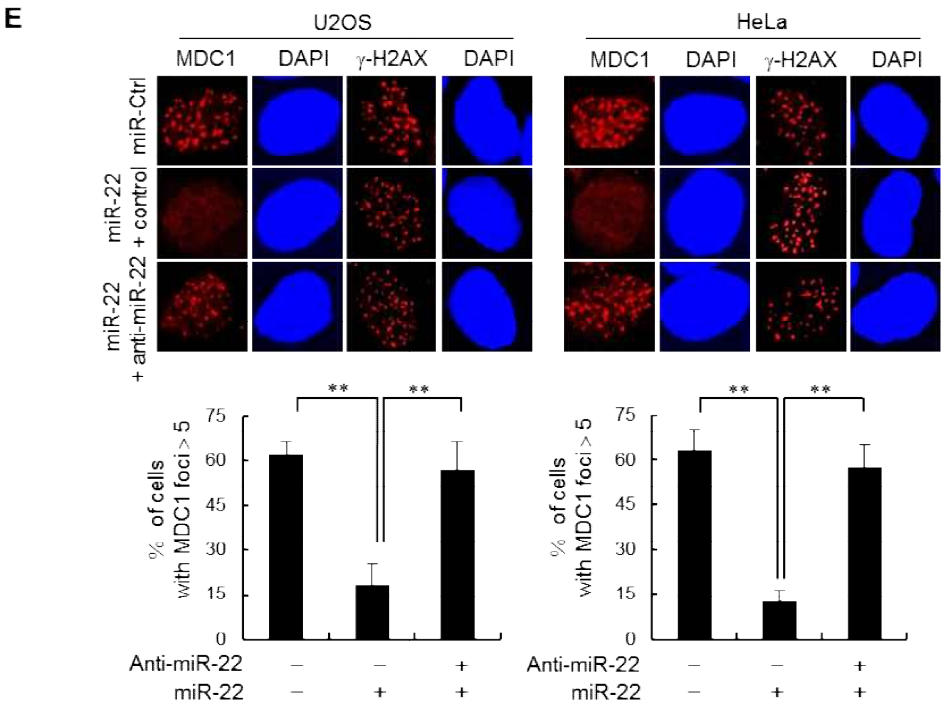

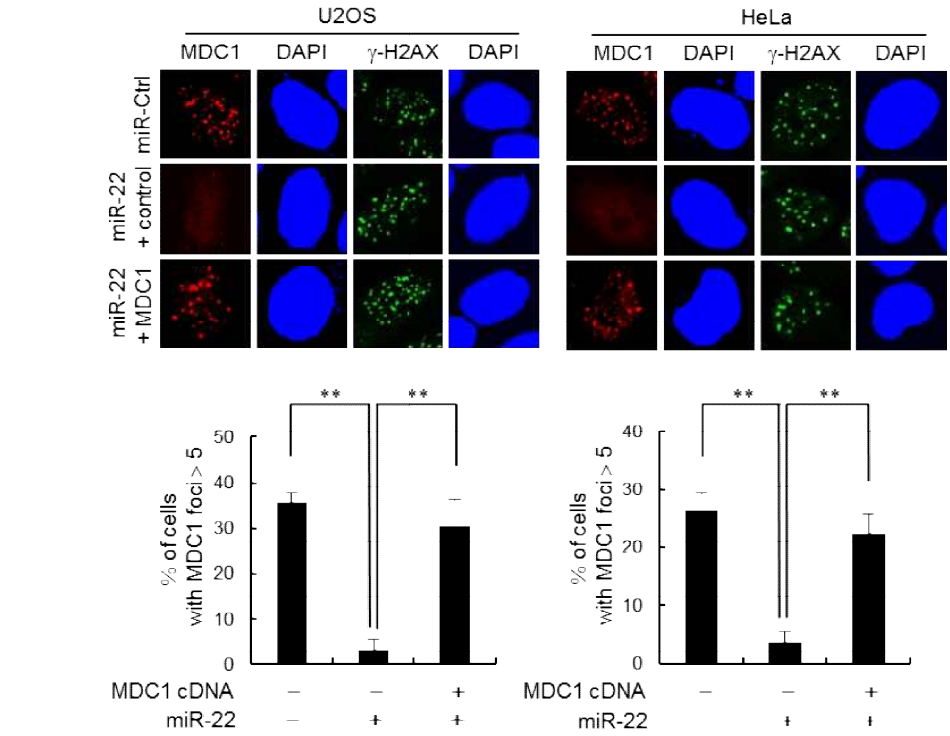

Figure 1 miR-22 directly affects MDC1 expression. (A) HEK293T cells were co-transfected with the MDC1 3 -UTR-luciferase reporter vector and the candidate miRNAs, which were predicted by at least five bioinformatics algo-rithms, or the miRNA negative control (miR-Ctrl). Luciferase activity was measured after 24 hr. Results are shown as means SD (n = 3). ** P < 0.01 (B) The levels of MDC1 protein were measured using western blotting in HEK293T cells transfected with the indicated miRNAs. (C) A schematic representation of MDC1 3 -UTR. The light red is the seed sequence of miR-22. Wild type 3 -UTR of MDC1 (MDC1 3 -UTR-wt) and 3'-UTR of MDC1 with a deletion of the miR-22 target site (MDC1 3 -UTR-mt) shown. (D) MDC1 3 -UTR-wt and MDC1 3 -UTR-mt were cotransfected with miR-22 (left) or pre-miR-22 (right) in HEK293T cells. Luciferase activity was measured 24 hr after the transfection.. (E, F) miR-22-expressing cells were transfected with anti-miR-22 (E) or miR-22-insensitive MDC1 (F) and were treated with 10 Gy of IR and

then fixed for immunofluorescence staining of MDC1 and −H2AX, 3 hr after IR. The lower histograms show the percentage of cells containing five distinct MDC1 foci per cells. At least 100 cells were analyzed for each treatment. Results in D−F are shown as means SD (n = 3). ** P < 0.01

Figure 2

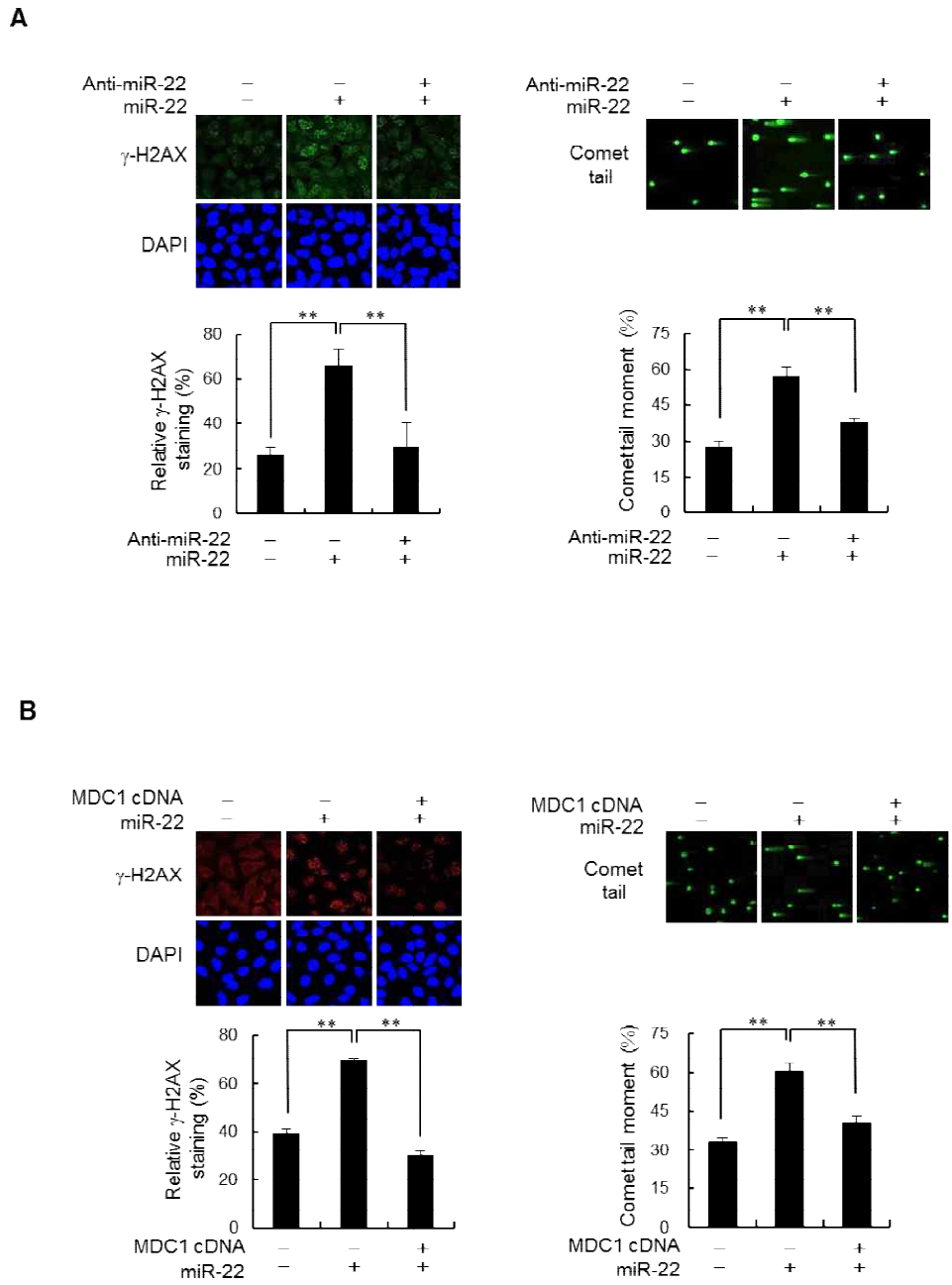

C

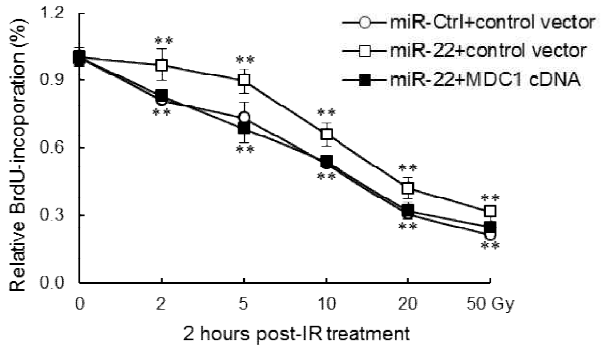

D

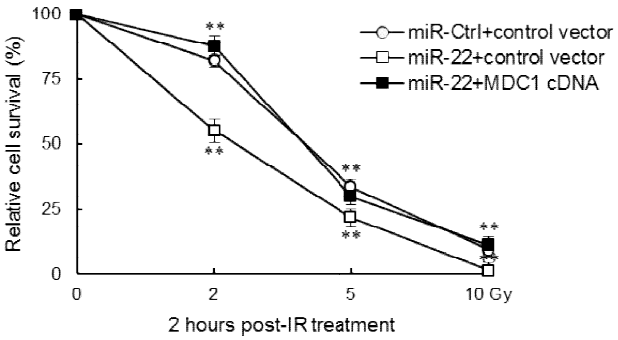

E

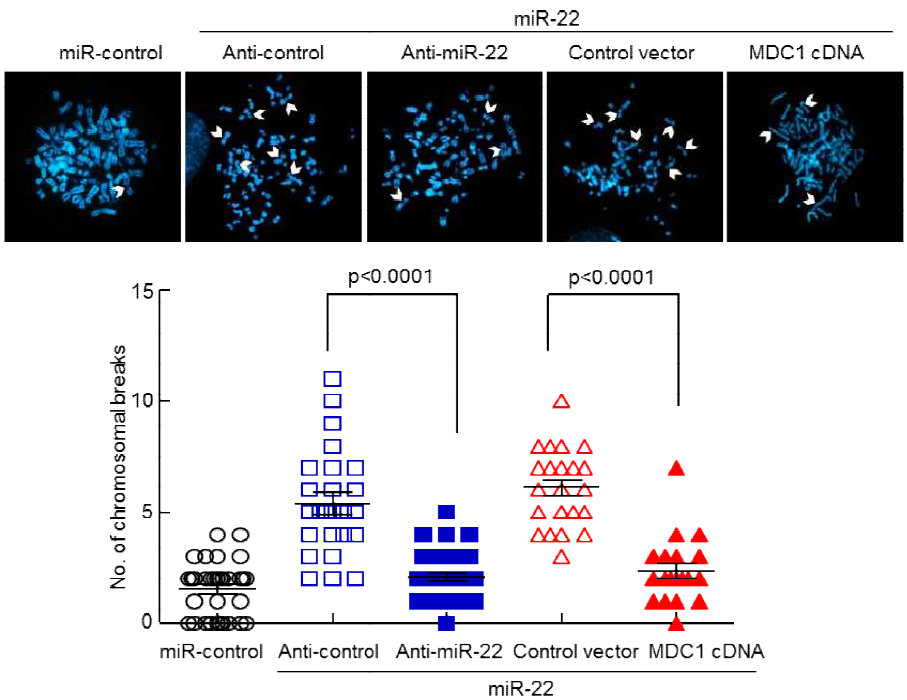

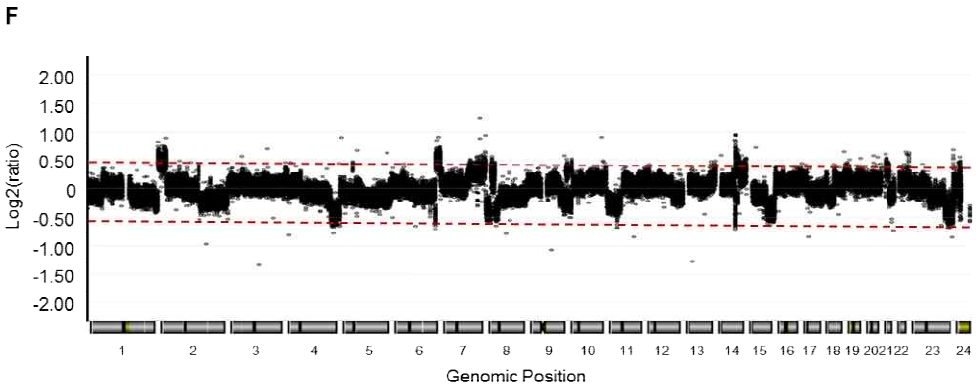

Figure 2 miR-22-mediated MDC1 down-regulation induces DNA damage. (A, B) miR-22-expressing U2OS cells were transfected with anti-miR-22 (A) or miR-22-insensitive MDC1 (B) and then irradiated with 10 Gy of IR. Cells were then analyzed by -H2AX staining sixteen hr after IR (left) and by comet assay three hr after IR (right). Representative images (the upper panel) and quantification (the lower panel) of unrepaired DSBs are shown. DAPI was used for nuclear staining. (C) BrdU incorporation was measured using a colorimetric assay after indicated doses of IR using U2OS cells transfected with indicated combinations of miRNAs and cDNA constructs. (D) Cell viabilities of indicated U2OS cells after indicated doses of IR were examined by the clonogenic survival assay.

(E) Representative images (the upper panel) and quantification (the lower panel) of chromosome breaks indicated cells exposed to IR. Arrows in panel indicate the chromosome breaks. (F) Array comparative genomic hybridization profiles of clones derived from GM00637 cells transfected with control miRNA or miR-22. Chromosomal regions above or below the red dotted line indicate amplifications or deletions of genomic positions, respectively. Results in A-E are shown as means SD (n = 3). ** P < 0.01

Figure 3

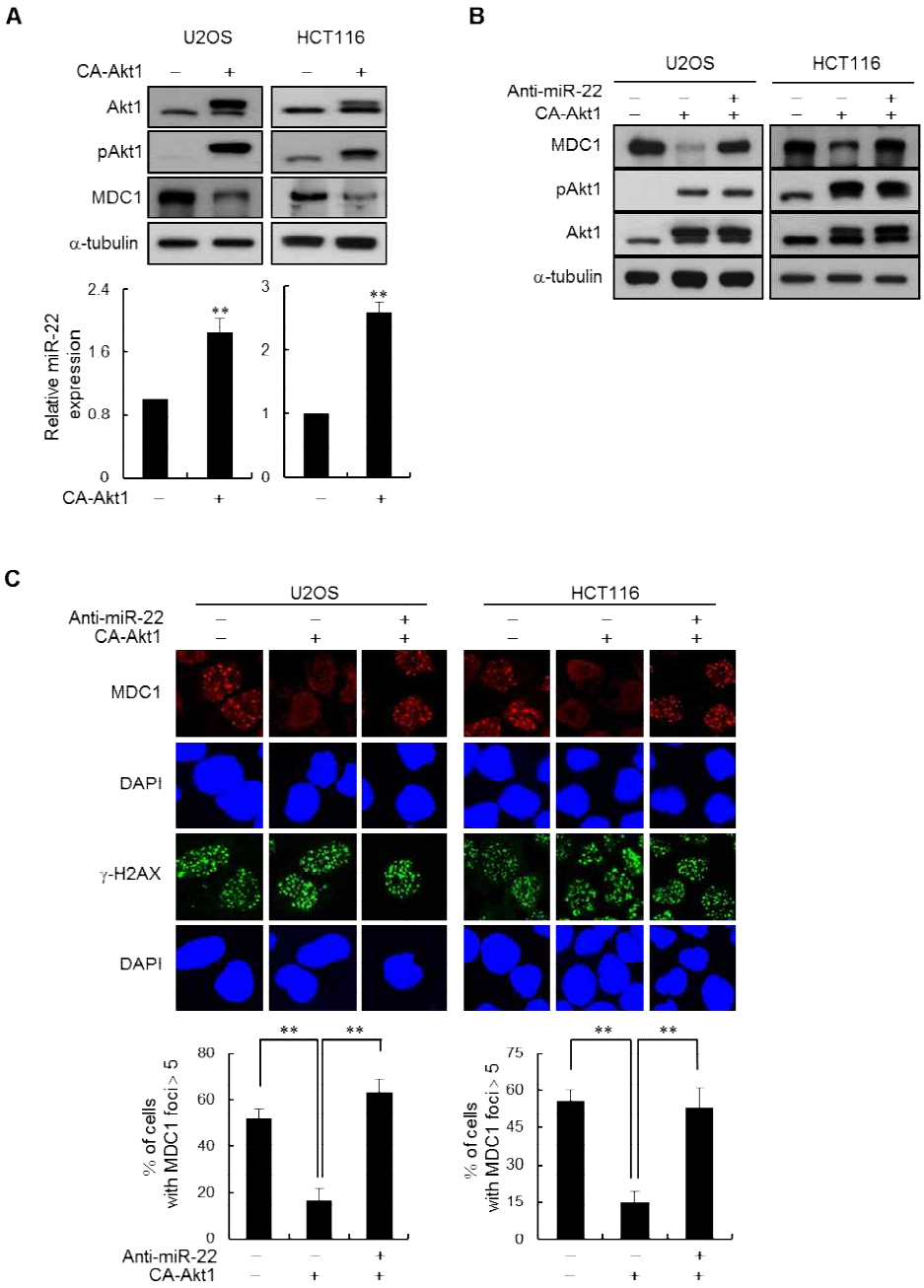

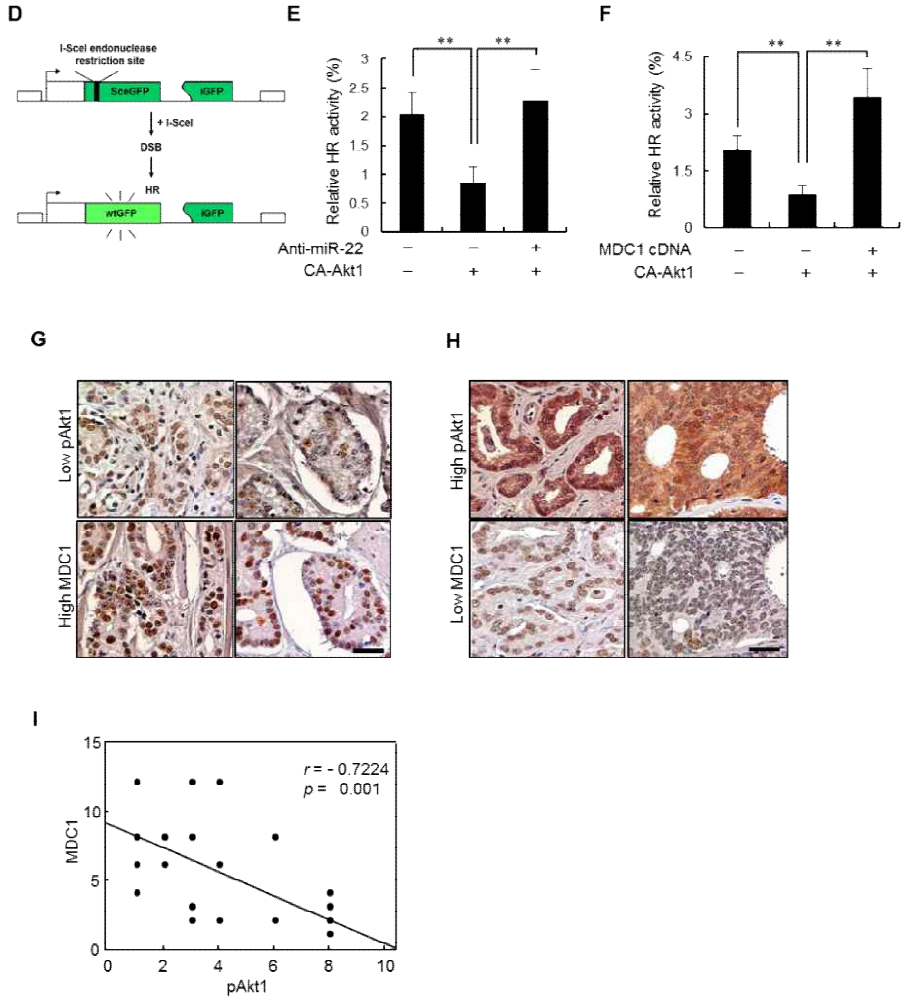

Figure 3 Oncogenic Akt1 leads to miR-22-mediated MDC1 deficiency and impairs HR. (A) Western blot analysis of MDC1 expression using cell extracts from con-trol vector- or CA-Akt1-transfected U2OS or HCT116 cells. miR-22 expres-

sion was quantitated using real-time qPCR. Results are shown as means SD (n = 3). ** P < 0.01. (B) miR-22-expressing cells were transfected with anti-miR-22. Two days after the transfection, the cell lysates were analyzed using western blotting with the indicated antibodies. (C) Representative images (the upper panel) and quantification (the lower panel) of IR (10 Gy)-induced MDC1 and -H2AX foci in cells cotransfected with anti-miR-22 and CA-Akt1 or with CA-Akt1 alone. Results are shown as means SD (n = 3). ** P < 0.01. (D) A schematic showing the assay for the fluorescence-based measurement of HR-mediated DSB repair. (E) U2OS DR-GFP cells were cotransfected with anti-miR-22 and CA-Akt1 or with CA-Akt1 alone and then infected with adenovirus encoding I-SceI. After 3 days, the percentage of cells expressing GFP was measured using flow cytometry. Results are shown as means SD (n = 3). ** P < 0.01. (F) The same experiments and quantitation described in (E) were performed using miR-22-insensitive MDC1 instead of anti-miR-22. Results are

shown as means SD (n = 3). ** P < 0.01. (G, H) Immunohistochemisty analysis for phospho-Akt1 (pAkt1) and MDC1 using a prostate tumor tissue array. Representative images of tumor specimens showing weak pAkt1 and strong MDC1 staining (G) or strong pAkt1 and weak MDC1 staining (H) are presented. Hematoxylin counterstain (blue color) was included for nuclei staining. The scale bar corresponds to 25 m. (I) A scatter plot showing the negative correlation between pAkt1 and MDC1 expression in the prostate cancer tissue microarray. The p-value and Pearson's correlation coefficient (r) are calculated.

Figure 4

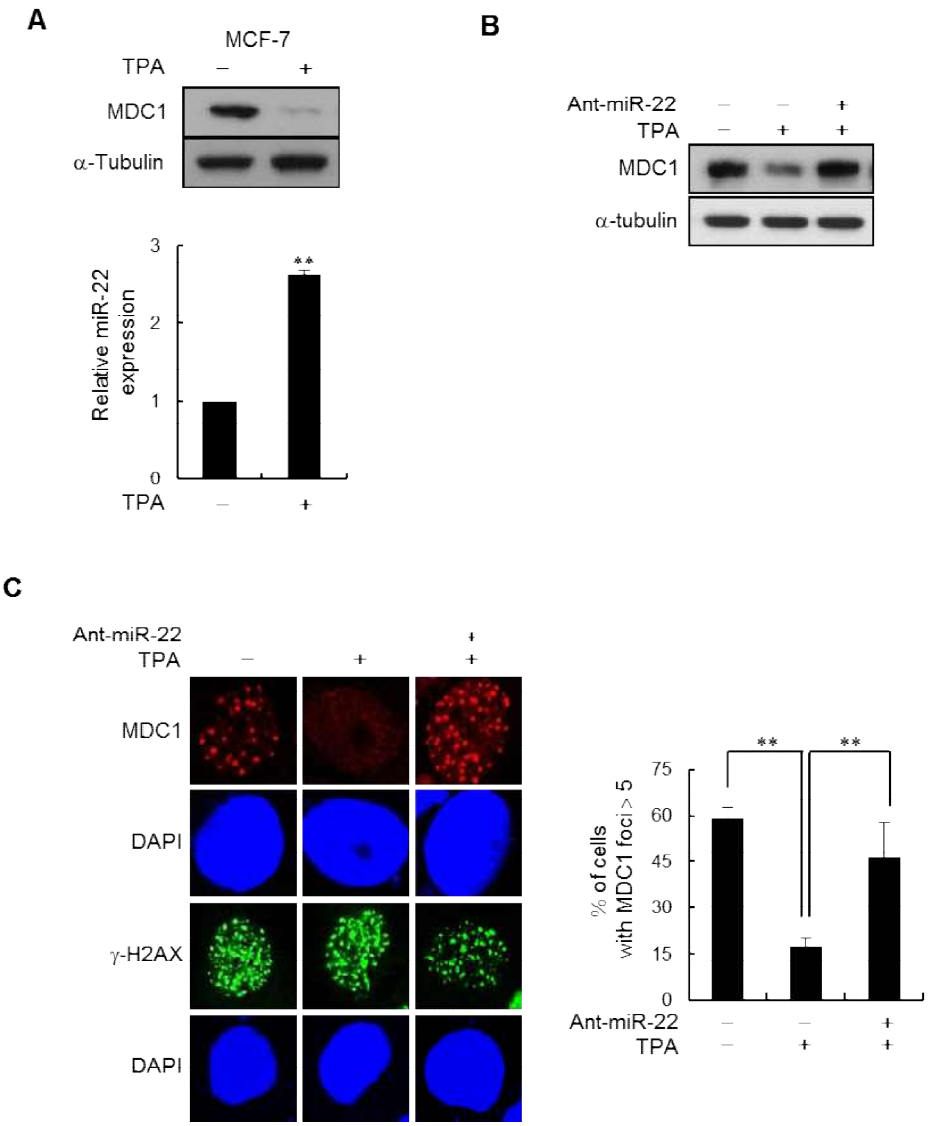

D

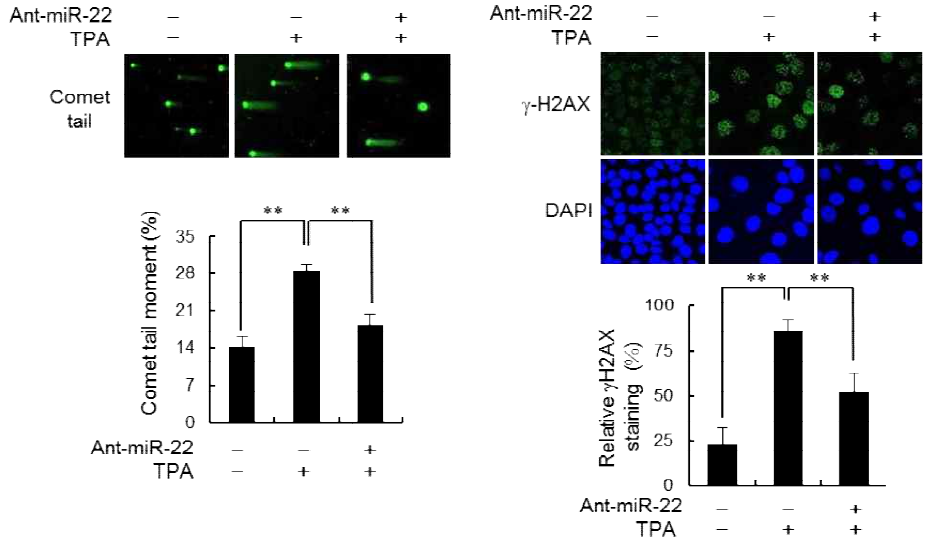

E

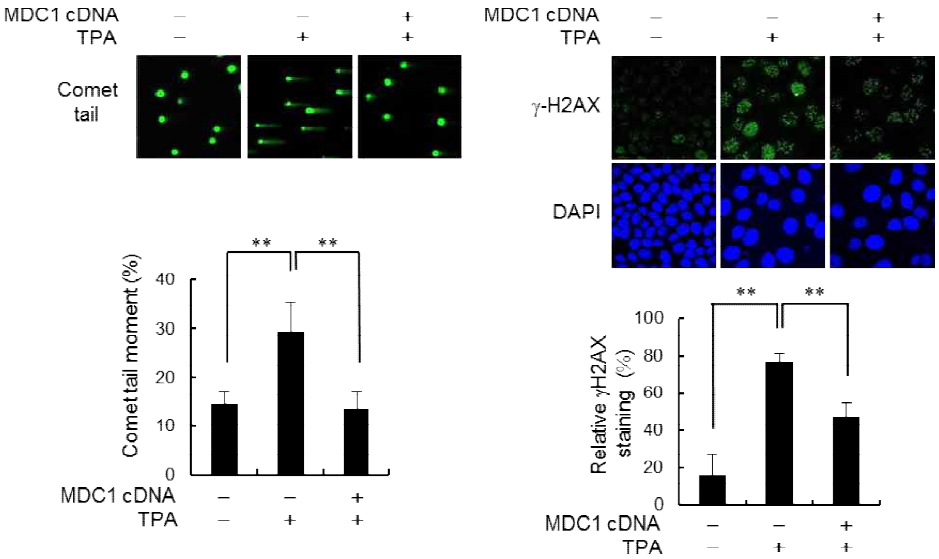

Figure 4 Cellular differentiation down-regulates MDC1 and affects DDR. (A) Western blot and real-time qPCR analysis for MDC1 and miR-22 expression in TPA-differentiated MCF-7 cells. Results are shown as means SD (n = 3). ** P < 0.01. (B) The levels of MDC1 protein were measured in TPA-treated MCF-7 cells in the absence or presence of anti-miR-22. (C) TPA-treated MCF-7 cells were transfected with anti-miR-22 and were treated with IR (10 Gy) and then fixed for immunofluorescence staining of MDC1 and -H2AX. The graph in the right panel shows the percentage of cells containing five distinct MDC1 foci per cells. (D, E) Transfection of TPA-treated MCF-7 cells with anti-miR-22 (D) or miR-22-insensitive MDC1 (E) rescues DSBs repair, as measured by the comet assay (left) and -H2AX staining (right). Representative images (the upper panel) and quantification (the lower panel) of unrepaired DSBs are shown. DAPI was used for nuclear staining. Results in C-E are shown as means SD (n = 3). ** P < 0.01.

Figure 5

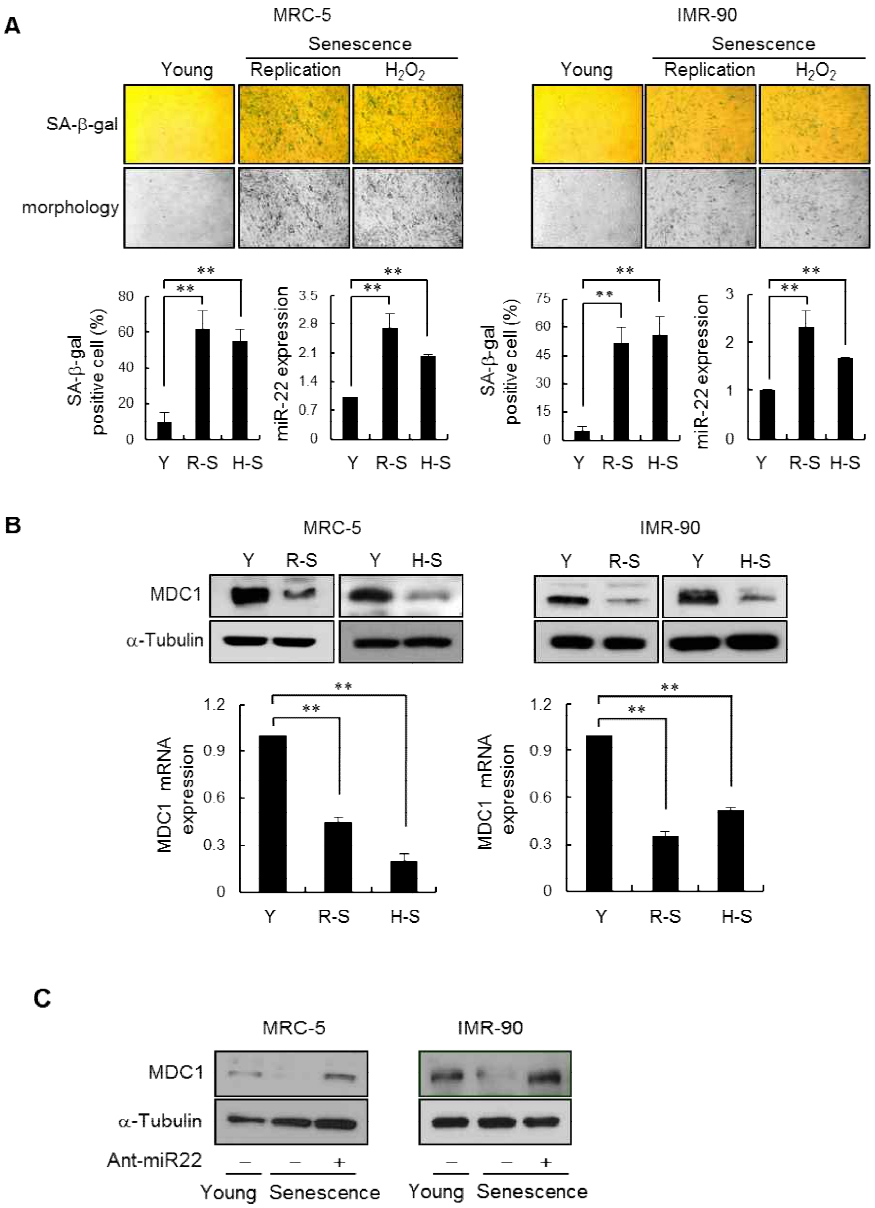

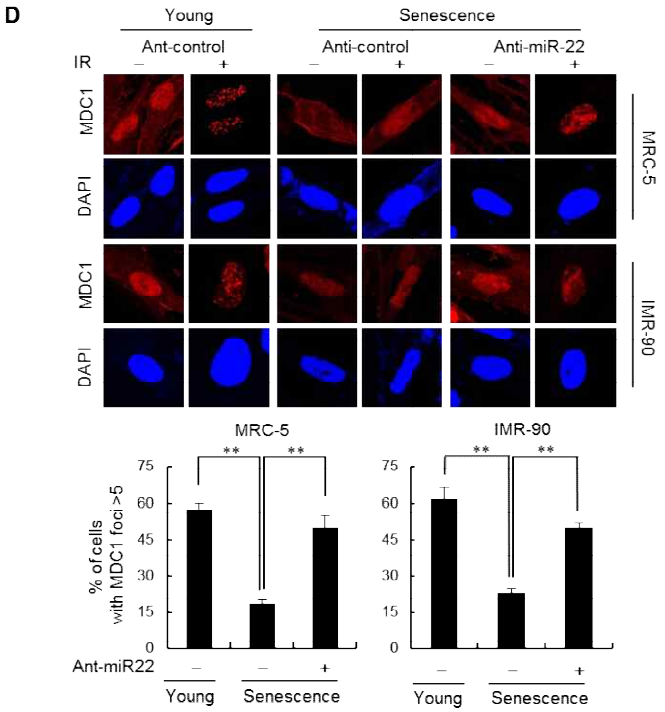

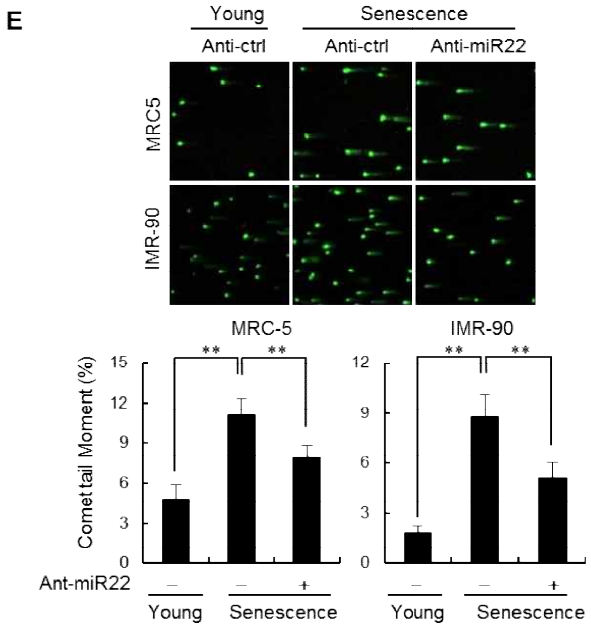

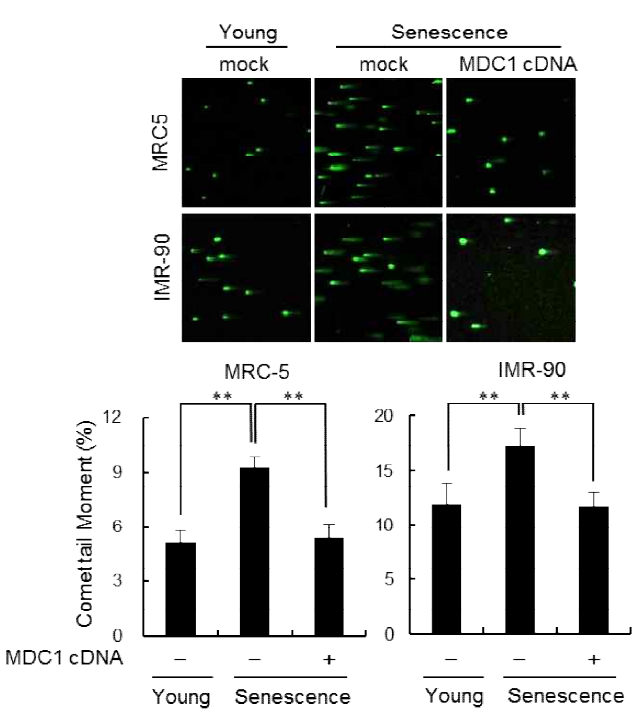

Figure 5 Cellular senescence up-regulates endogenous miR-22 and inhibits DSB repair. (A) Senescence in MRC-5 and IMR-90 cells was induced by either serial passage (replicative senescence: R-S) or through treatment with H2O2 (H2O2-induced premature senescence: H-S). Representative images for cell morpholo-gy and SA- -gal activity in young (Y) and senescent cells are shown. The lower histograms show the percentage of SA- -gal-positive cells (left) and

miR-22 levels (right). Results are shown as means SD (n = 3). ** P < 0.01. (B) Representative western blot analysis of MDC1 in young (Y), replicative senescent (R-S), and H2O2-induced premature senescent (H-S) cells. MDC1 mRNA was measured using real-time qPCR. Results are shown as means SD (n = 3). ** P < 0.01. (C) Rescue of MDC1 expression level by transfecting anti-miR-22 into H2O2-induced premature senescent cells. (D) MDC1 foci formation in young and H2O2-induced premature senescent cells, with and without IR treatment and with and without anti-miR-22. The lower histograms show the percentage of cells containing five distinct MDC1 foci per cells. (E, F) Transfection of H2O2-induced premature senescent cells with anti-miR-22 (E) or miR-22-insensitive MDC1 cDNA (F) increased DSB repair upon IR exposure, as measured by the comet assay. Representative images are shown in upper panel and quantitation of average tail length is below. Results in D-F are shown as means SD (n = 3). ** P < 0.01.

Figure 6

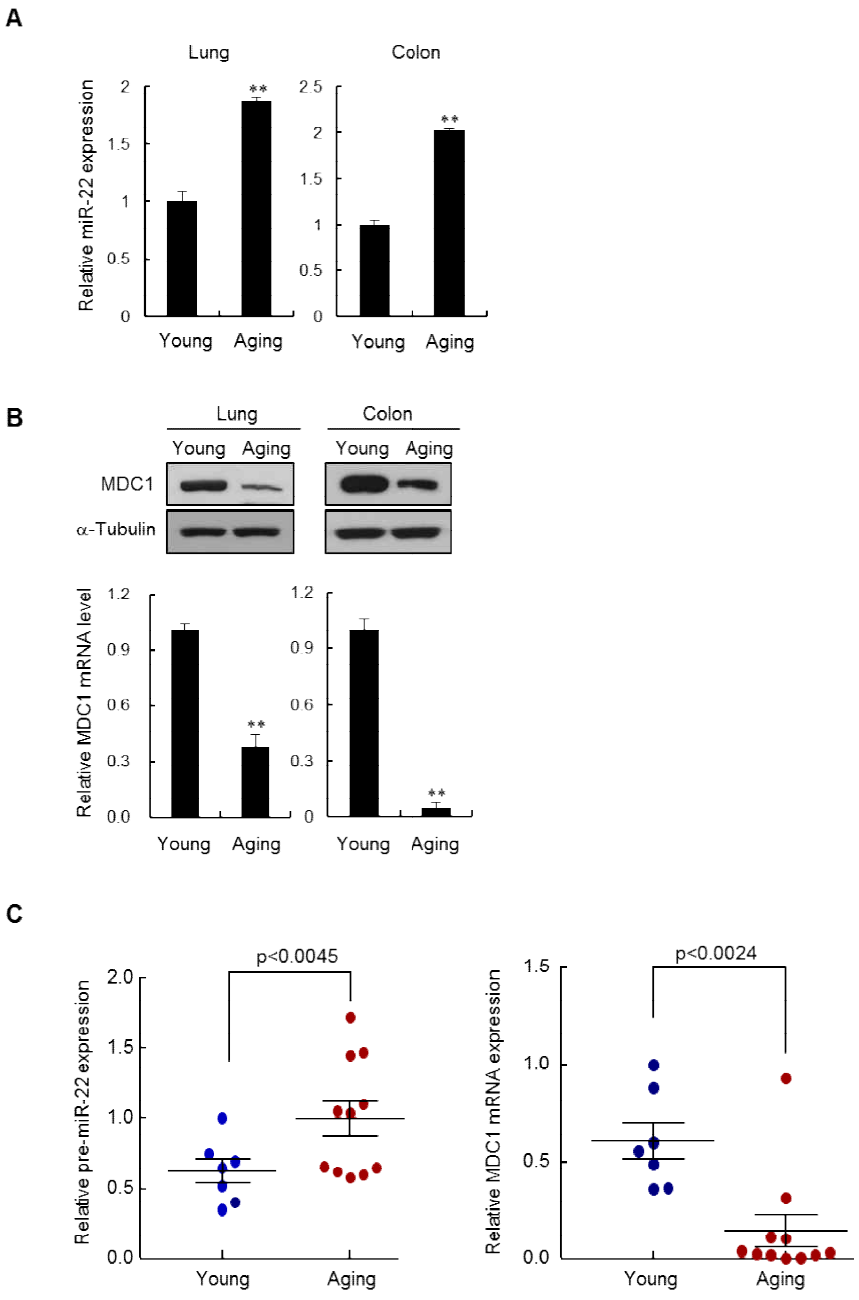

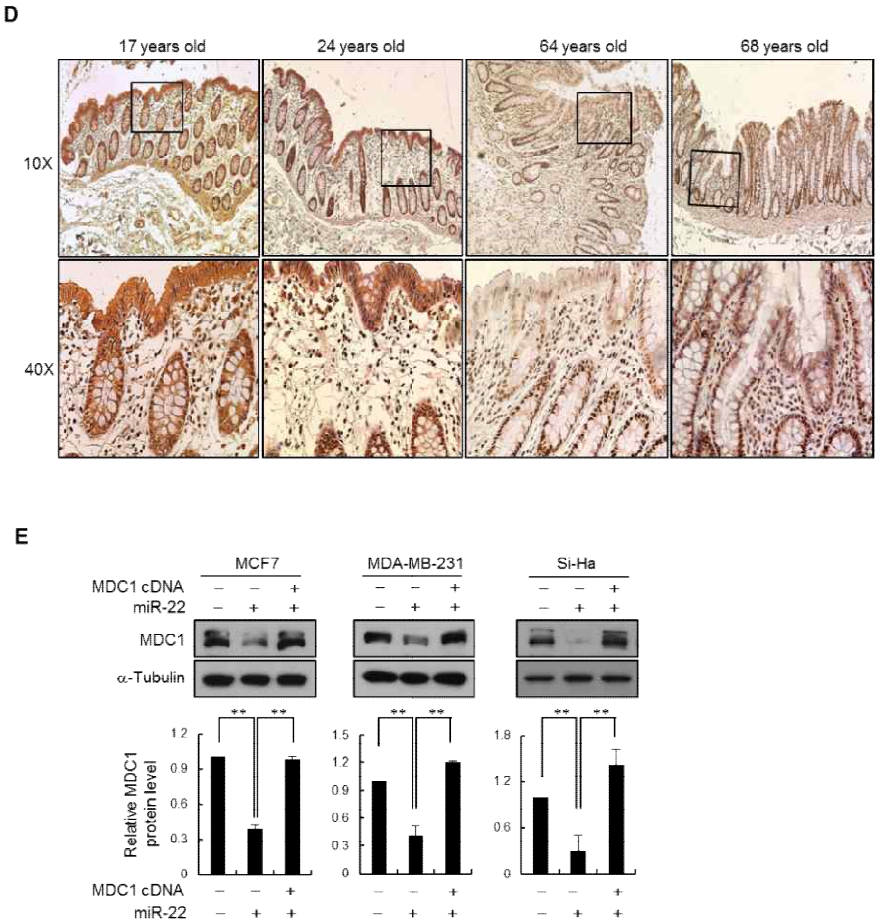

Figure 6 miR−22 represses MDC1 expression and affects genome integrity in aging cells. (A) Expression of miR−22 was measured using lung and colon tissues collected from young (6 months) and old (23 months) mice. Results are shown as means SD (n = 3). ** P < 0.01. (B) Expression of MDC1 protein and mRNA was measured using lung and colon tissues extracts from young and old mice.

Results are shown as means SD (n = 3). ** P < 0.01. (C) Expression of pre-miR-22 and MDC1 mRNA was measured using peripheral blood mononuclear cells of young (below 25 years) and old (above 65 years) donors. (D) Immunohistochemical staining of MDC1 in colon biopsies from young and old donors. The images in the bottom panel (40 X) are the magnified images of boxed regions in the top panel (10 X). (E) The level of MDC1 protein was measured in MCF7, MDA-MB-231, and Si-Ha cells transfected with miR-22 or together with miR-22 and MDC1. The bottom panel shows the quantitation of western blot analysis. Results are shown as means SD (n = 3). ** P < 0.01. (F) miR-22-induced senescent cancer cells are defective in DSB repair as shown by increased -H2AX staining. miR-22-insensitive MDC1 expression decreased -H2AX staining. Representative images are shown in upper panel and quantitation of unrepaired of DSBs is below. Results are shown as means SD (n = 3). ** P < 0.01.

Figure 7

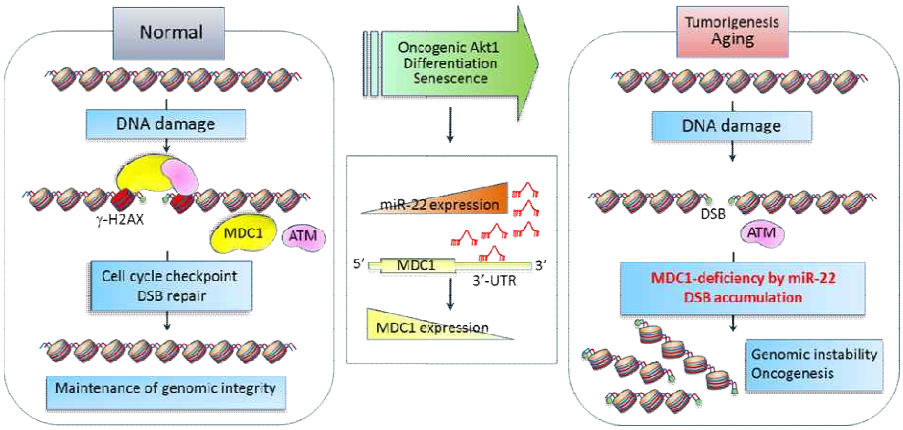

Figure 7 A model for the role of miR-22 in genomic instability. Under normal conditions, DNA damage recruits MDC1 to the damaged DNA sites and the recruitment initiates DDR. This cascade is central in maintaining genomic integrity. During differentiation, senescence, or activation of oncogenic Akt1, miR-22 is up-regulated and its cellular target protein MDC1 is decreased. A deficiency of MDC1, caused by miR-22, impairs DDR and unrepaired DSBs accumulate. This regulatory network exists in aging and tumorigenesis. Thus, regulation of miR-

22 and MDC1 expression upon various pathophysiological contexts is a key process in modulating genomic instability.

DISCUSSION

DSBs are dangerous DNA lesions that cause mutations and genomic rearrangements and consequently contribute to tumorigenesis. DSB repair is therefore an essential way for cells to maintain genome stability and to prevent cancer (1, 2, 36). MDC1 plays a central role in DDR by orchestrating DSB repair and checkpoint activation (3). Therefore, either malfunction or loss of MDC1 is directly linked to genomic instability. In this study, we investigated a mechanism by which MDC1 expression is regulated and found that a particular microRNA, miR-22, modulates MDC1 regulation at the post-transcriptional level by targeting the 3 -UTR of MDC1 mRNA. Our results highlight miR-22 as a key regulator of DDR function of MDC1. To date, there are no roles described for miR-22 in normal cells. Endogenous miR-22 expression appears to be dependent on particular abnormal physiological contexts, including high Akt1 activity, differentiation, and replicative/stress-induced senescence.

Akt is a serine/threonine kinase, which is a key downstream target of the signaling pathway mediated by phosphotide-3 kinase (PI3K), and plays a pivotal role in the regulation of diverse cellular process, including cell growth, proliferation, and survival (37). Aberrant activation of the PI3K/Akt pathway is a common event in a wide range of human cancers (38). Accumulated evidence supports a role of Akt as an important modulator of DNA damage checkpoint signaling and DSB repair (39-41). As the most hazardous of DNA lesions, DSBs lead to genome rearrangement and cell death following exposure to genotoxic stressors (Khanna and Jackson, 2001). At least two mechanisms exist for the repair of DSBs, HR, and NHEJ. HR is an error-free repair pathway, whereas NHEJ is error-prone (36, 42). Activated Akt stimulates NHEJ repair, which contributes to chemo- or radioresistance in some tumor cells with constitutive Akt activation (43-45). In contrast, activation of Akt inhibits HR due to suppression of the DDR under pathologic circumstances (21, 46). Because defective HR can lead to ge-

nome instability and predisposition to cancer (36), the inhibition of HR by the activation of Akt may contribute to tumorigenesis. However, the precise mecha-nism by which activated Akt exerts its influence on HR needs to be elucidated. In the present study, we detected a decline in HR in cells expressing constitutively active Akt. This decline in HR was associated with the upregulation of miR-22, which caused the loss of MDC1 function. These results also showed that both the inhibition of miR-22 and overexpression of MDC1 completely restored the func-tion of MDC1 in the DDR and HR in cancer cells with high Akt activity. This sce-nario clarifies how elevated Akt1 activity might increase genomic instability and foster an environment for cancer development. Remarkably, this inverse corre-lation between pAkt1 and MDC1 expression occurs in vivo in human prostate tu-mor tissues. Thus, miR-22-mediated MDC1 down-regulation could be an un-derlying mechanism behind Akt1-mediated oncogenesis and anti-miR-22 may be a new potential therapeutic agent for Akt-induced tumorigenesis.

Terminally differentiated cells are characterized by permanent withdrawal from the cell cycle and do not replicate their genomes. Although the majority of cells in multicellular organisms are terminally differentiated and do not prolifer-ate, most studies on the DDR have investigated the response of proliferating cells to genotoxic agents. Thus, little information exists on the effect of DNA damage in terminally differentiated cells. A common feature seems to be that while resistance to various genotoxic stressors increases during the course of cellular differentiation, DNA repair is progressively attenuated, and therefore, terminally differentiated cells can conceivably accumulate numerous lesions in its genome (47, 48). However, the molecular mechanisms for the attenuation of DNA repair in terminally differentiated cells are not well understood. In some cases, specific repair proteins are downregulated at the transcriptional level (49) or functional DDR signaling is impaired (50, 51). Recently, It has been reported that the miR-24 family is upregulated during differentiation of hematopoietic

cells and directly downregulates H2AX expression to inhibit DNA repair and enhance chemosensitivity (14), suggesting that miRNAs might be novel players regulating DDR in differentiate cells. Our study shows a strong correlation between the loss of MDC1 function and miR-22 up-regulation in terminally differentiated MCF-7 cells. Intriguingly, MDC1 expression is also suppressed in terminally differentiated astrocytes before and after exposure to IR (50). Because miR-22 is upregulated in various postmitotic cells (14, 25, 26), the down-regulation of MDC1 by miR-22 could be a key factor impairing DSB repair in differentiated cells.

Cellular senescence is a status of permanent proliferative arrest resulting either from telomere shortening after multiple rounds of cell division (replicative senescence) or from various stressors, such as oncogenes or oxidative stress (stress-induced premature senescence) (31). During cellular senescence or organismal aging, mammalian cells accumulate mutations in their genome and often

end up with abnormal chromosomal rearrangements (52). These mutations and genomic rearrangements arise from aberrant DSB repair. For example, senescent cells contain more DSBs and reduced NHEJ repair than non-senescent cells (53). Stem cells accumulate DNA damage as they age and are defective in NHEJ repair (54, 55). HR-mediated repair decreases sharply during aging in replicatively senescent cells (30). Thus, the miR-22-mediated decrease in MDC1 expression that occurs during cellular senescence explains how senescent cells become defective in DSB repair capacity. Interestingly, H2O2 and BU-induced premature senescence also showed the same expression pattern change for miR-22 and MDC1, which may explain how environmental factors play a role in the regulation of genomic instability, and this may be true for factors besides oxidative stress. In all of these cases, our model provides a representative mo-lecular mechanism for how environmental stress or the progressive history of cells, tissues or organisms can affect genome integrity.

The incidence of carcinoma, the most common cancer in humans, increases exponentially with age (56). This is most likely due to the mutations and genomic rearrangements that accumulate during normal aging, and which could contribute to the transformation of functionality in aged tissues (29). For example, in patients with Hutchinson-Gilford progeria syndrome, a genetic condition characterized by the rapid appearance of aging, a positive correlation is observed between tumorigenesis and senescence with a high frequency of mutations (57). Hence, cellular senescence is a potent tumor-suppressing mechanism but at the same time, it also contributes to cancer promotion at an advanced age (31). miR-22 has been proposed to be a tumor suppressor because it could inhibit cell proliferation and induce a senescence-like phenotype in human breast, cervical, and colon cancer cells (28, 32, 35). We observed the senescence-like phenotype when we overexpressed miR-22 in human cancer cells; however, we also found that miR-22 induced extensive DSB accumulation in the same cells. Fur-

thermore, our in vivo data using both mouse and human tissues strongly suggest a positive correlation between miR-22 up-regulation and MDC1-deficiency. Thus, even though miR-22-induced senescence may act as a barrier to cancer development, the defects in DDR and DSB repair that result from the downstream effects of miR-22 regulation cause detrimental chromosomal abnormalities, leading to the accumulation of secondary insults that might establish a cellular environment fostering tumorigenesis and cancer progression independent of proliferation-related phenotypes, and this may provide an underlying molecular mechanism for initiation of cancer development. This hypothesis is supported by the recent finding that miR-22 has an oncogenic functions (58, 59).

Herein, we have shown that miR-22 is a key player in DSB repair and genomic stability through modulation of MDC1 expression under particular pathophysiological contexts, including high Akt1 activity, differentiation, and replicative/stress-induced senescence. In mice, MDC1 knockout leads to compromised

genomic stability and induces tumorigenesis (4, 5). However, there are no reports whether inefficient DSB repair and chromosome aberration occur as a result of reduced levels of MDC1 in human pathology. Our findings reveal the miR-22/MDC1 interaction as a previously unsuspected link between MDC1 function under aberrant physiological conditions, and they expand our understanding of MDC1-mediated cellular functions contributing to the maintenance of genomic stability in Akt-activated cells, during differentiation, and cellular senescence (Figure 7). Antagonists of endogenous miR-22 in these cells may thus be useful therapeutic strategies for enhancing MDC1 expression, given that it could block dysregulated DDR, accumulated DNA damage and chromosomal abnormalities.

ABSTRACT

The study of the microRNA –induced cellular senescence

Man Jin Cha

Advisor : Prof. Ho Jin You, M.M. &Ph.D.

Department of Pharmacology,

Graduate school of Chosun University

MDC1 functions as a platform to assemble repair proteins at the damaged DNA sites. Although loss of MDC1 results in genomic instability and tumorigenicity, the molecular mechanisms controlling MDC1 expression are currently unknown. Here, we found that microRNA-22 (miR-22) suppresses MDC1 expression, and as a consequence, causes an impaired DNA damage response, decreased DNA double-strand break (DSB) repair and genomic instability. Several intracellular physiological states, including Akt1 activation, differentiation, and senescence,

hinder MDC1-initiated DSB repair by up-regulating endogenous miR-22. Importantly, a negative correlation between miR-22 and MDC1 expression was observed in both tumors and aged tissues, suggesting that miR-22-induced genomic instability is a general phenomenon. Cancer cells that overexpressed miR-22 accumulated a significant number of DSB, regardless of their senescence phenotype. Thus, our findings define miR-22 as an oncogenic master regulator of MDC1 expression and suggest a molecular mechanism for how quiescent cells or aged tissues increase genomic instability, fostering an environment that promotes tumorigenesis.

REFERENCES

1. Ciccia A, and Elledge SJ. The DNA damage response: making it safe to play with knives. Mol Cell. 2010;40(2):179-204.

2. Jackson SP, and Bartek J. The DNA-damage response in human biology and disease. Nature. 2009;461(7267):1071-8.

3. Huen MS, and Chen J. Assembly of checkpoint and repair machineries at DNA damage sites. Trends Biochem Sci. 2010;35(2):101-8.

4. Lou Z, Minter-Dykhouse K, Franco S, Gostissa M, Rivera MA, Celeste A, Manis JP, van Deursen J, Nussenzweig A, Paull TT, et al. MDC1 maintains genomic stability by participating in the amplification of ATM-dependent DNA damage signals. Mol Cell. 2006;21(2):187-200.

5. Minter-Dykhouse K, Ward I, Huen MS, Chen J, and Lou Z. Distinct versus overlapping functions of MDC1 and 53BP1 in DNA damage response and tumorigenesis. J Cell Biol. 2008;181(5):727-35.

6. Bartkova J, Horejsi Z, Sehested M, Nesland JM, Rajpert-De Meyts E, Skakkebaek NE, Stucki M, Jackson S, Lukas J, and Bartek J. DNA damage response mediators MDC1 and 53BP1: constitutive activation and aberrant loss in breast and lung cancer, but not in testicular germ cell tumours. Oncogene. 2007;26(53):7414-22.

7. Galanty Y, Belotserkovskaya R, Coates J, and Jackson SP. RNF4, a SUMO-targeted ubiquitin E3 ligase, promotes DNA double-strand break repair. Genes Dev. 2012;26(11):1179-95.

8. Luo K, Zhang H, Wang L, Yuan J, and Lou Z. Sumoylation of MDC1 is important for proper DNA damage response. EMBO J. 2012;31(13):3008-19.

9. Yin Y, Seifert A, Chua JS, Maure JF, Golebiowski F, and Hay RT. SUMO-targeted ubiquitin E3 ligase RNF4 is required for the response of human cells to DNA damage. Genes Dev. 2012;26(11):1196-208.

10. Bartel DP. MicroRNAs: genomics, biogenesis, mechanism, and function.

Cell. 2004;116(2):281-97.

11. Chowdhury D, Choi YE, and Brault ME. Charity begins at home: non-coding RNA functions in DNA repair. Nature reviews Molecular cell biology. 2013;14(3):181-9.

12. Hu H, Du L, Nagabayashi G, Seeger RC, and Gatti RA. ATM is down-regulated by N-Myc-regulated microRNA-421. Proc Natl Acad Sci U S A. 2010;107(4):1506-11.

13. Moskwa P, Buffa FM, Pan Y, Panchakshari R, Gottipati P, Muschel RJ, Beech J, Kulshrestha R, Abdelmohsen K, Weinstock DM, et al. miR-182-mediated downregulation of BRCA1 impacts DNA repair and sensitivity to PARP inhibitors. Mol Cell. 2011;41(2):210-20.

14. Lal A, Pan Y, Navarro F, Dykxhoorn DM, Moreau L, Meire E, Bentwich Z, Lieberman J, and Chowdhury D. miR-24-mediated downregulation of H2AX suppresses DNA repair in terminally differentiated blood cells. Nat Struct Mol

Biol. 2009;16(5):492-8.

15. Francia S, Michelini F, Saxena A, Tang D, de Hoon M, Anelli V, Mione M, Carninci P, and d'Adda di Fagagna F. Site-specific DICER and DROSHA RNA products control the DNA-damage response. Nature. 2012;488(7410):231-5.

16. Zhang J, Ma Z, Treszezamsky A, and Powell SN. MDC1 interacts with Rad51 and facilitates homologous recombination. Nat Struct Mol Biol. 2005;12(10):902-9.

17. Dimitrova N, and de Lange T. MDC1 accelerates nonhomologous end-joining of dysfunctional telomeres. Genes Dev. 2006;20(23):3238-43.

18. Goldberg M, Stucki M, Falck J, D'Amours D, Rahman D, Pappin D, Bartek J, and Jackson SP. MDC1 is required for the intra-S-phase DNA damage checkpoint. Nature. 2003;421(6926):952-6.

19. Lou Z, Minter-Dykhouse K, Wu X, and Chen J. MDC1 is coupled to activated CHK2 in mammalian DNA damage response pathways. Nature.

2003;421(6926):957-61.

20. Stewart GS, Wang B, Bignell CR, Taylor AM, and Elledge SJ. MDC1 is a mediator of the mammalian DNA damage checkpoint. Nature. 2003;421(6926):961-6.

21. Plo I, Laulier C, Gauthier L, Lebrun F, Calvo F, and Lopez BS. AKT1 inhibits homologous recombination by inducing cytoplasmic retention of BRCA1 and RAD51. Cancer Res. 2008;68(22):9404-12.

22. Bar N, and Dikstein R. miR-22 forms a regulatory loop in PTEN/AKT pathway and modulates signaling kinetics. PLoS One. 2010;5(5):e10859.

23. Poliseno L, Salmena L, Riccardi L, Fornari A, Song MS, Hobbs RM, Sportoletti P, Varmeh S, Egia A, Fedele G, et al. Identification of the miR-106b~25 microRNA cluster as a proto-oncogenic PTEN-targeting intron that cooperates with its host gene MCM7 in transformation. Science signaling. 2010;3(117):ra29.

24. Weinstock DM, Nakanishi K, Helgadottir HR, and Jasin M. Assaying double-strand break repair pathway choice in mammalian cells using a targeted endonuclease or the RAG recombinase. Methods Enzymol. 2006;409(524-40.

25. Choong ML, Yang HH, and McNiece I. MicroRNA expression profiling during human cord blood-derived CD34 cell erythropoiesis. Exp Hematol. 2007;35(4):551-64.

26. Gangaraju VK, and Lin H. MicroRNAs: key regulators of stem cells. Nat Rev Mol Cell Biol. 2009;10(2):116-25.

27. Valette A, Gas N, Jozan S, Roubinet F, Dupont MA, and Bayard F. Influence of 12-O-tetradecanoylphorbol-13-acetate on proliferation and maturation of human breast carcinoma cells (MCF-7): relationship to cell cycle events. Cancer Res. 1987;47(6):1615-20.

28. Xu D, Takeshita F, Hino Y, Fukunaga S, Kudo Y, Tamaki A, Matsunaga J, Takahashi RU, Takata T, Shimamoto A, et al. miR-22 represses cancer pro-

gression by inducing cellular senescence. The Journal of cell biology. 2011;193(2):409-24.

29. Lombard DB, Chua KF, Mostoslavsky R, Franco S, Gostissa M, and Alt FW. DNA repair, genome stability, and aging. Cell. 2005;120(4):497-512.

30. Mao Z, Tian X, Van Meter M, Ke Z, Gorbunova V, and Seluanov A. Sirtuin 6 (SIRT6) rescues the decline of homologous recombination repair during replicative senescence. Proc Natl Acad Sci U S A. 2012;109(29):11800-5.

31. Campisi J. Senescent cells, tumor suppression, and organismal aging: good citizens, bad neighbors. Cell. 2005;120(4):513-22.

32. Tsuchiya N, Izumiya M, Ogata-Kawata H, Okamoto K, Fujiwara Y, Nakai M, Okabe A, Schetter AJ, Bowman ED, Midorikawa Y, et al. Tumor suppressor miR-22 determines p53-dependent cellular fate through post-transcriptional regulation of p21. Cancer research. 2011;71(13):4628-39.

33. Patel JB, Appaiah HN, Burnett RM, Bhat-Nakshatri P, Wang G, Mehta R,

Badve S, Thomson MJ, Hammond S, Steeg P, et al. Control of EVI-1 oncogene expression in metastatic breast cancer cells through microRNA miR-22. Oncogene. 2011;30(11):1290-301.

34. Xiong J, Du Q, and Liang Z. Tumor-suppressive microRNA-22 inhibits the transcription of E-box-containing c-Myc target genes by silencing c-Myc binding protein. Oncogene. 2010;29(35):4980-8.

35. Alvarez-Diaz S, Valle N, Ferrer-Mayorga G, Lombardia L, Herrera M, Dominguez O, Segura MF, Bonilla F, Hernando E, and Munoz A. MicroRNA-22 is induced by vitamin D and contributes to its antiproliferative, antimigratory and gene regulatory effects in colon cancer cells. Human molecular genetics. 2012;21(10):2157-65.

36. Moynahan ME, and Jasin M. Mitotic homologous recombination maintains genomic stability and suppresses tumorigenesis. Nat Rev Mol Cell Biol. 2010;11(3):196-207.

37. Cantley LC. The phosphoinositide 3-kinase pathway. Science. 2002;296(5573):1655-7.

38. Luo J, Manning BD, and Cantley LC. Targeting the PI3K-Akt pathway in human cancer: rationale and promise. Cancer Cell. 2003;4(4):257-62.

39. Henry MK, Lynch JT, Eapen AK, and Quelle FW. DNA damage-induced cell-cycle arrest of hematopoietic cells is overridden by activation of the PI-3 kinase/Akt signaling pathway. Blood. 2001;98(3):834-41.

40. Wanzel M, Kleine-Kohlbrecher D, Herold S, Hock A, Berns K, Park J, Hemmings B, and Eilers M. Akt and 14-3-3eta regulate Miz1 to control cell-cycle arrest after DNA damage. Nat Cell Biol. 2005;7(1):30-41.

41. Hirose Y, Katayama M, Mirzoeva OK, Berger MS, and Pieper RO. Akt activation suppresses Chk2-mediated, methylating agent-induced G2 arrest and protects from temozolomide-induced mitotic catastrophe and cellular senescence. Cancer Res. 2005;65(11):4861-9.

42. Lieber MR, Ma Y, Pannicke U, and Schwarz K. Mechanism and regulation of human non-homologous DNA end-joining. Nat Rev Mol Cell Biol. 2003;4(9):712-20.

43. Golding SE, Morgan RN, Adams BR, Hawkins AJ, Povirk LF, and Valerie K. Pro-survival AKT and ERK signaling from EGFR and mutant EGFRvIII enhances DNA double-strand break repair in human glioma cells. Cancer Biol Ther. 2009;8(8):730-8.

44. Kao GD, Jiang Z, Fernandes AM, Gupta AK, and Maity A. Inhibition of phosphatidylinositol-3-OH kinase/Akt signaling impairs DNA repair in glioblastoma cells following ionizing radiation. J Biol Chem. 2007;282(29):21206-12.

45. Toulany M, Kehlbach R, Florczak U, Sak A, Wang S, Chen J, Lobrich M, and Rodemann HP. Targeting of AKT1 enhances radiation toxicity of human tumor cells by inhibiting DNA-PKcs-dependent DNA double-strand break repair.

Mol Cancer Ther. 2008;7(7):1772-81.

46. Xu N, Hegarat N, Black EJ, Scott MT, Hochegger H, and Gillespie DA. Akt/PKB suppresses DNA damage processing and checkpoint activation in late G2. J Cell Biol. 2010;190(3):297-305.

47. Nouspikel T, and Hanawalt PC. DNA repair in terminally differentiated cells. DNA repair. 2002;1(1):59-75.

48. Fortini P, and Dogliotti E. Mechanisms of dealing with DNA damage in terminally differentiated cells. Mutat Res. 2010;685(1-2):38-44.

49. Narciso L, Fortini P, Pajalunga D, Franchitto A, Liu P, Degan P, Frechet M, Demple B, Crescenzi M, and Dogliotti E. Terminally differentiated muscle cells are defective in base excision DNA repair and hypersensitive to oxygen injury. Proc Natl Acad Sci U S A. 2007;104(43):17010-5.

50. Schneider L, Fumagalli M, and d'Adda di Fagagna F. Terminally differen-tiated astrocytes lack DNA damage response signaling and are radioresistant but

retain DNA repair proficiency. Cell Death Differ. 2012;19(4):582-91.

51. Fortini P, Ferretti C, Pascucci B, Narciso L, Pajalunga D, Puggioni EM, Castino R, Isidoro C, Crescenzi M, and Dogliotti E. DNA damage response by single-strand breaks in terminally differentiated muscle cells and the control of muscle integrity. Cell Death Differ. 2012;19(11):1741-9.

52. Vijg J, and Suh Y. Genome instability and aging. Annu Rev Physiol. 2013;75(645-68.

53. Seluanov A, Mittelman D, Pereira-Smith OM, Wilson JH, and Gorbunova V. DNA end joining becomes less efficient and more error-prone during cellular senescence. Proc Natl Acad Sci U S A. 2004;101(20):7624-9.

54. Nijnik A, Woodbine L, Marchetti C, Dawson S, Lambe T, Liu C, Rodrigues NP, Crockford TL, Cabuy E, Vindigni A, et al. DNA repair is limiting for haema-topoietic stem cells during ageing. Nature. 2007;447(7145):686-90.

55. Rossi DJ, Bryder D, Seita J, Nussenzweig A, Hoeijmakers J, and

Weissman IL. Deficiencies in DNA damage repair limit the function of haemato-poietic stem cells with age. Nature. 2007;447(7145):725-9.

56. Carreca I, Balducci L, and Extermann M. Cancer in the older person. Cancer Treat Rev. 2005;31(5):380-402.

57. Martien S, and Abbadie C. Acquisition of oxidative DNA damage during senescence: the first step toward carcinogenesis? Ann N Y Acad Sci. 2007;1119(51-63.

58. Song SJ, Poliseno L, Song MS, Ala U, Webster K, Ng C, Beringer G, Brikbak NJ, Yuan X, Cantley LC, et al. MicroRNA-antagonism regulates breast cancer stemness and metastasis via TET-family-dependent chromatin remod-eling. Cell. 2013;154(2):311-24.

59. Song SJ, Ito K, Ala U, Kats L, Webster K, Sun SM, Jongen-Lavrencic M, Manova-Todorova K, Teruya-Feldstein J, Avigan DE, et al. The oncogenic mi-croRNA miR-22 targets the TET2 tumor suppressor to promote hematopoietic

stem cell self-renewal and transformation. Cell Stem Cell. 2013;13(1):87-101.

60. Lee JH, Kang Y, Khare V, Jin ZY, Kang MY, Yoon Y, Hyun JW, Chung MH, Cho SI, Jun JY, et al. The p53-inducible gene 3 (PIG3) contributes to early cel-lular response to DNA damage. Oncogene. 2010;29(10):1431-50.